J. Am. Chem. Soc. 1987, 109, 3287-3297

H-Atom Transfer between Metal Complex Ions in Solution

Robert A. Binstead[†] **and Thomas J. Meyer***

Contribution from the Department of Chemistry, University of North Carolina, Chapel Hill, North Carolina 27514.

Received August 25, 1986

Abstract: The reaction between $[Ru^{IV}(bpy)_2(py)(O)]^{2+}$ and $[Ru^{II}(bpy)_2(py)(OH_2)]^{2+}$ in H_2O to form 2 equiv of $[Ru^{III}(bpy)_2(py)(OH)]^{2+}$ occurs with a solvent isotope effect of $(k_{H_2O}/k_{D_2O})^{25 °C} = 16.1 \pm 0.2$ both in neat solvent and at $I = 0.10$ M (Na_2SO_4). The rate of the reaction is independent of pH for 2 < pH < 9 but decreases at pH >9, where the Ru(II) aqua complex becomes deprotonated to form the hydroxo complex, $[Ru^{II}(bpy)_2(py)(OH)]^+$ ($pK_b = 3.20 \pm 0.05$). The rate constants for the two pathways at $T = 25$ °C and $I = 0.10$ M are $k_{H_2O} = (2.174 \pm 0.028) \times 10^5$ M^{-1} s^{-1} and $k_{OH} = (0.247 \pm 0.024) \times 10^5$ M^{-1} s^{-1}. The solvent isotope effect is much smaller for the second pathway with $(k_{OH}/k_{OD})^{25 °C} = 1.5$. The large kinetic isotope effect for the k_{H_2O} pathway and the observation of a linear dependence of k_{H_2O} on mole fraction of deuterium suggest that the mechanism involves the *simultaneous* transfer of a *proton* and an *electron* from $Ru^{II}–OH_2$ to $Ru^{IV}=O$. Complementary kinetics studies on the cross reaction between $[Ru^{III}(trpy)(bpy)(OH)]^{2+}$ and $[Ru^{II}(bpy)_2(py)(OH_2)]^{2+}$ have revealed a significant kinetic isotope effect of $(k_{H_2O}/k_{D_2O})^{25 °C} = 5.8 \pm 0.4$, which also displays a linear dependence on mole fraction of deuterium. The rate of the cross reaction is independent of pH for 3 < pH < 8 with $k_{H_2O} = (4.1 \pm 0.2) \times 10^5$ M^{-1} s^{-1} ($T = 25$ °C, $I = 0.005$ M). For pH >9 a second pathway with $[Ru^{II}(bpy)_2(py)(OH)]^+$ as the reductant dominates the kinetics and there is a *dramatic increase* in the observed rate, giving the extrapolated estimates, $k_{OH} = (4.4 \pm 0.3) \times 10^7$ M^{-1} s^{-1} and $k_{OD} \simeq (2.9) \times 10^7$ M^{-1} s^{-1}. In the pathway at high pH there is no difference in H^+ content between reactants and products and the reaction occurs by outer-sphere electron transfer.

Electrochemical studies have shown that aqua-polypyridyl complexes of Ru and Os have an extensive higher oxidation state chemistry,[1-8] e.g., Scheme I, where the key to the accessibility of the higher oxidation states is the loss of protons upon oxidation and stabilization of the higher oxidation states by electron donation from bound hydroxo or oxo ligands. The higher oxidation states of Ru have proven to be remarkable stoichiometric and catalytic oxidants.[8-13] The results of mechanistic studies suggest that in carrying out such reactions the Ru oxidants take advantage of a variety of pathways based on the Ru^{IV}-oxo group including O-atom transfer, H-atom transfer, and hydride transfer.

Scheme I

$$(bpy)_2(py)Ru^{II}—OH_2{}^{2+} \xrightarrow[-H^+]{-e^-} (bpy)_2(py)Ru^{III}—OH^{2+} \xrightarrow[-H^+]{-e^-} (bpy)_2(py)Ru^{IV}=O^{2+}$$

(at pH 7; bpy is 2,2′-bipyridine; py is pyridine)

In order to understand the mechanistic consequences of changes in proton content on redox reactions and to begin to assess these factors determining which of a series of possible pathways will be favored for a given reaction, we report here the results of kinetic studies on two relatively simple reactions. The first (eq 1) is a comproportionation reaction between $Ru^{IV}=O$ and $Ru^{II}—OH_2$,

$$(bpy)_2(py)Ru^{IV}=O^{2+} + (bpy)_2(py)Ru^{II}—OH_2{}^{2+} \rightarrow 2(bpy)_2(py)Ru^{III}\text{-}OH^{2+} \quad (1)$$

and the second (eq 2) is a cross reaction, where, because of the differences in coordination environments, there is a small driving force, $\Delta E°' = 0.056$ V, $\Delta G° = -1.3$ kcal mol^{-1}. Part of this work has appeared in a preliminary communication.[14]

$$(trpy)(bpy)Ru^{III}\text{-}OH^{2+} + (bpy)_2(py)Ru^{II}—OH_2{}^{2+} \rightarrow (trpy)(bpy)Ru^{II}—OH_2{}^{2+} + (bpy)_2(py)Ru^{III}—OH^{2+} \quad (2)$$

Experimental Section

Materials. Water of conductivity grade ($R \geq 16$ MΩ) and deuterium oxide, D_2O, of 99.8% g-atom purity (Aldrich GOLD LABEL) were used for the electrochemical and kinetics measurements. Ionic strength was maintained with use of sodium sulfate, Na_2SO_4, which had been recrystallized once from distilled water. Analytical reagent grade sodium borate, $Na_2B_4O_7\cdot 10H_2O$, sodium hydrogen phosphate, $Na_2HPO_4\cdot 7H_2O$, potassium dihydrogen phosphate, KH_2PO_4, sodium hydroxide, NaOH, sodium deuteroxide, NaOD (Aldrich, 99%+), and sulfuric acid, H_2SO_4, were used without further purification to maintain pH/pD. Chemical oxidations were performed with ceric ammonium nitrate, $(NH_4)_2[Ce(NO_3)_6]$ (G.F.Smith). Lithium perchlorate, $LiClO_4\cdot 3H_2O$, was recrystallized three times from distilled water and dried at 110 °C over P_2O_5 to yield $LiClO_4\cdot H_2O$ for use as a supporting electrolyte.

Syntheses. $[Ru(trpy)(bpy)OH_2](ClO_4)_2$ was prepared, purified, and characterized as described previously.[2a]

$[Ru(bpy)_2(py)OH_2](PF_6)_2\cdot H_2O$ was prepared by photolysis[15] of a solution containing 0.1 g of $[Ru(bpy)_2(py)_2](Cl)_2$ ($\lambda_{max} = 452$ nm) in 40 mL of 0.1 M H_2SO_4. The reaction was monitored spectrophotometrically until completion and then a saturated aqueous solution of NH_4PF_6 was added dropwise to precipitate the crude product. The crude product was collected by filtration, washed with distilled water, and air dried. The sample was recrystallized from hot, distilled water, collected by filtration, and washed with distilled water and diethyl ether followed by drying in vacuo over P_2O_5. The final product was characterized by UV-vis spectrophotometry: $\lambda_{max} = 470$ nm, $\epsilon = 8800$ M^{-1} cm^{-1} (cf. lit. $\epsilon_{470} = 8400$ M^{-1} cm^{-1} via a different synthetic route).[1]

$[Ru(bpy)_2(py)O](PF_6)_2$ was prepared from the Ru(II) complex by stoichiometric oxidation with cerium(IV) ion in 1 M $HClO_4$ as described previously,[1] except that a solution of NH_4PF_6 was added dropwise to precipitate the product. The product was collected by filtration, washed with distilled water, and then recrystallized from hot distilled water,

---

[†] Present address: Chemistry Department, Naval Research Laboratories, Washington, DC 20036.

(1) Moyer, B. A.; Meyer, T. J. *Inorg. Chem.* **1981**, *20*, 436.

(2) (a) Takeuchi, K. J.; Thompson, M. S.; Pipes, D. W.; Meyer, T. J. *Inorg. Chem.* **1984**, *23*, 1845. (b) McHatton, R. C.; Anson, F. S. *Inorg. Chem.* **1984**, *23*, 3935.

(3) Che, C. M.; Wong, K. Y.; Leung, W. H.; Poon, C. W. *Inorg. Chem.* **1986**, *25*, 345.

(4) Pipes, D. W.; Meyer, T. J. *J. Am. Chem. Soc.* **1984**, *106*, 7653.

(5) (a) Takeuchi, K. J.; Samuels, G. J.; Gersten, S. W.; Gilbert, J. A.; Meyer, T. J. *Inorg. Chem.* **1983**, *22*, 1407. (b) Dobson, J. C.; Takeuchi, K. J.; Pipes, D. W.; Geselowitz, D. A.; Meyer, T. J. *Inorg. Chem.* **1986**, *25*, 2357.

(6) Che, C. M.; Wong, K. Y. *J. Chem. Soc., Chem. Commun.* **1986**, 229.

(7) Diamantis, A. A.; Murphy, W. R., Jr.; Meyer, T. J. *Inorg. Chem.* **1984**, *23*, 3230.

(8) (a) Gilbert, J. A.; Eggleston, D. S.; Murphy, W. R., Jr.; Geselowitz, D. A.; Gersten, S. W.; Hodgson, D. J.; Meyer, T. J. *J. Am. Chem. Soc.* **1985**, *107*, 3855. (b) Gilbert, J. A.; Geselowitz, D.; Meyer, T. J. *J. Am. Chem. Soc.* **1986**, *108*, 1493. (c) Doppelt, P.; Meyer, T. J. *Inorg. Chem.*, in press.

(9) Meyer, T. J. *J. Electrochem. Soc.* **1984**, *131*, 221C.

(10) (a) Moyer, B. A.; Thompson, M. S.; Meyer, T. J. *J. Am. Chem. Soc.* **1980**, *102*, 2310. (b) Thompson, M. S.; De Giovani, W. F.; Moyer, B. A.; Meyer, T. J. *J. Org. Chem.* **1984**, *49*, 4972.

(11) (a) Thompson, M. S.; Meyer, T. J. *J. Am. Chem. Soc.* **1982**, *104*, 4106. (b) Thompson, M. S.; Meyer, T. J. *Ibid.* **1982**, *104*, 5070.

(12) Vining, W. J.; Meyer, T. J. *J. Electroanal. Chem.* **1985**, *195*, 183.

(13) (a) Che, C. M.; Cheng, W. K.; Mak, T. C. W. *J. Chem. Soc., Chem. Commun.* **1986**, 200. (b) Dobson, J. C.; Seok, W. K.; Meyer, T. J. *Inorg. Chem.* **1986**, *25*, 1514.

(14) Binstead, R. A.; Moyer, B. A.; Samuels, G. J.; Meyer, T. J. *J. Am. Chem. Soc.* **1981**, *103*, 2897.

(15) Durham, B.; Walsh, J. L.; Carter, C. L.; Meyer, T. J. *Inorg. Chem.* **1980**, *19*, 860.

0002-7863/87/1509-3287\$01.50/0 © 1987 American Chemical Society

collected as above and dried in vacuo over P_2O_5. Samples were characterized by UV spectrophotometry.[1]

Measurements. Routine UV-vis spectra were obtained in 1-cm silica cuvettes (Nippon Seiki Glass) with either a Bausch and Lomb Spectronic 210 or a Varian 634 spectrophotometer fitted with thermostated cell holders. Precision measurements for the spectrophotometric titration of $[Ru(bpy)_2(py)(OH_2)]^{2+}$ vs. $[OH^-]$ were performed on a Cary 17I instrument interfaced at 10 bit precision with a Commodore 4032 microcomputer system and a Hewlett-Packard 7470A digital plotter. The spectra were smoothed with use of a quartic polynomial least-squares routine[16b] prior to extraction of single wavelength absorbance vs. pH data at the peak maxima 335.5, 364.5, 470, and 506 nm. A total of 14 spectra were obtained over the pH range 6.6–12.88, using volumetric dilutions from stock solutions of NaOH, Na_2SO_4, and the Ru(II) complex in CO_2-free distilled water.

The pH of solutions used for kinetics measurements was determined with a Radiometer Model 62 pH meter and type C glass electrode vs. SCE after calibration with standard buffers at 25 °C. The spectrophotometric titration of $[Ru(bpy)_2(py)(OH_2)]^{2+}$ vs. $[OH^-]$ at an ionic strength of 0.10 M (Na_2SO_4) was performed with a Radiometer Model 28 pH meter with Ross type pH electrodes (Orion) after calibration with Merck Titrisol buffers in CO_2-free distilled water. To avoid measurement errors above pH 10 with the sodium ion electrolytes, calibration curves of pH_{meas} vs. pOH were determined over the range 10^{-4} to 10^{-1} M NaOH at an ionic strength of 0.10 M (Na_2SO_4) and fitted to a quadratic polynomial by nonlinear least-squares regression,[16b] yielding an accurate measure of pOH. To correct measurements below pH 10 to pOH the value of pK_w must be known. The value of pK_w for Na_2SO_4 media has been determined by Akerlof at a number of concentrations.[17] These data were interpolated to 0.03333 M Na_2SO_4 (I = 0.10 M) by a quadratic fit for the nearest three measurements, yielding a value of $pK_w = 13.747$ at 25 °C. Values of pOH obtained from pH_{meas} and the pK_w agreed well with those calculated from the calibration curve. For D_2O solutions pOD was determined directly with use of volumetric dilutions from a stock solution of NaOD in D_2O, calibrated by titration with HCl obtained by volumetric dilution from freshly opened 12.23 M HCl. The pOD values based on dilution were checked by using the pH meter with use of the relationship $pD = pH_{meas} + 0.4$.[18]

Electrochemical measurements were made with either a Princeton Applied Research Model 173 or a custom made operational amplifier based potentiostat in conjunction with a custom made triangle wave generator,[19] and Au disk working electrode, a platinum wire auxiliary electrode, and a saturated sodium chloride calomel reference electrode (SSCE). The electrochemical cell was a three-compartment type with medium porosity glass frit separators, thermostated by immersion in a Colora WK-5 water bath. The reference electrode remained at room temperature (21–23 °C). Prior to each experiment the Au disk working electrode was polished with 0.25 μm diamond paste on microcloth (Buehler), rinsed with distilled water, and then pretreated by cycling past the anodic and cathodic limits in 0.01 M H_2SO_4. Controlled potential bulk electrolysis was performed by using the same cell arrangement with Pt gauze working and auxiliary electrodes and the SSCE reference electrode in conjunction with a P.A.R. 173/179 coulometry system. Electrolysis was terminated after the calculated number of coulombs had been passed and the background current had fallen below 1% of the initial current.

Kinetics measurements were made on an Aminco-Morrow Stopped-Flow apparatus attached to a Beckman DU monochromator under pseudo-first-order conditions (10-fold excess). The temperature of the reactant solutions was measured by using a calibrated thermistor (Omega) deeply embedded between the drive syringes in the thermostating block of the stopped-flow apparatus. For measurements away from room temperature the Teflon/quartz observation cell, which is not well thermostated in this apparatus, was flushed several times to ensure temperature equilibration of the system before acquisition of data. The transmission decay traces from the photomultiplier tube were converted to absorbance decays with use of a logarithmic amplifier of our design based on an Analog Devices 757P module and then conditioned by an operational amplifier based filter circuit with selectable time constant, which was set to 0.1 × the observed decay time. The resulting exponential traces were acquired in digital form by using a Biomation Model 1010 waveform recorder and either replotted on a Hewlett-Packard Model 7015B X–Y chart recorder and then manually entered into a Commodore microcomputer via a Hewlett-Packard 7470A digital plotter in digitizing mode or entered directly into the microcomputer via an IEEE-488 interface to the Biomation 1010. In either case the kinetics traces were fitted first by linear least-squares regression as $\log_e (A - A_\infty)$ vs. time with the Commodore microcomputer over a range of 2.5 to 3 half-lives to obtain the pseudo-first-order rate constant, k_{obsd} (s^{-1}).

The comproportionation reaction (eq 1) was followed at 470 nm after mixing equal volumes of 2×10^{-4} M $[Ru^{II}(bpy)_2(py)(OH_2)]^{2+}$ ($\epsilon = 8800$ $M^{-1}\,cm^{-1}$) and 2×10^{-5} M $[Ru^{IV}(bpy)_2(py)(O)]^{2+}$ ($\epsilon \simeq 300$ $M^{-1}\,cm^{-1}$) both in neat aqueous solution and in buffer/Na_2SO_4 electrolyte ($I = 0.10$ M) over the range 2 < pH < 10. Above pH 10 the reaction was followed at 505 nm, a maximum for $[Ru^{II}(bpy)_2(py)(OH)]^+$ ($\epsilon = 8330$ $M^{-1}\,cm^{-1}$), in a medium of NaOH/Na_2SO_4 ($I = 0.10$ M). For D_2O solutions the pD range was restricted to 6–13, with the use of NaOD/Na_2SO_4 electrolyte ($I = 0.10$ M). Since the Ru(IV) complex was not stable for long periods in alkaline solution, due to self-oxidation of the ligands,[20] the Ru(IV) solutions were prepared in 0.0333 M Na_2SO_4 solution and the Ru(II) complex in the buffer solution. The pH was measured both before and after mixing the Ru(II) and Ru(IV) solutions to obtain the pOH value as described above. The values of pOH for pH > 10 compared very well with calculated values of free $[OH^-]$ using the value of $pK_b = 3.20$ for $[Ru^{II}(bpy)_2(py)(OH)]^+$ determined spectrophotometrically (see below) and the total concentration of NaOH. The fitted pseudo-first-order decay curves gave correlation coefficients in the range 0.9995–0.99995.

The kinetics analysis for the comproportionation reaction (eq 1), a second-order reversible system of the type

$$A + B \underset{k_f}{\overset{k_r}{\rightleftharpoons}} 2C$$

$$K_{com} = \frac{k_f}{k_r} = \frac{[C]^2}{[A][B]}$$

could be simplified under the conditions used ($[A]_0 = 10[B]_0$) as an irreversible pseudo-first-order decay, neglecting k_r, for the range 2 < pH < 9, where $K_{com} \simeq 72$,[1] since the reaction was driven to >99% completion. Within this pH range the second-order rate constant, k' ($\simeq k_f$), was calculated with use of eq 3, where the molar concentration of the species in excess, $[A]_{ex}$, was calculated at the midpoint concentration of the absorbance range fitted in order to minimize the errors in the pseudo-first-order approximation (±5%). The midpoint concentration was

$$k' = k_{obsd}/[A]_{ex} \tag{3}$$

calculated from the initial concentration, the total absorbance change, the calibrated path length, and the extinction coefficient difference at the wavelength of observation.

For pH >9 the value of K_{com} decreases with increasing pH (see below). For example, at pH 12.6, where the value of $K_{com} \simeq 1$, the pseudo-first-order conditions used resulted in only 75% completion of the reaction. By using the Runge–Kutta algorithm[16b] to solve the differential rate equation numerically for $K_{com} = 1$ and $[A]_0 = 10[B]_0$, the concentration decay curve was found to be almost perfectly exponential with $k' \simeq 1.5k_f$ [Note: for $K_{com} = 4$ the $A + B \rightleftharpoons 2C$ system gives perfect exponential decays with $k' = 1.1k_f$, regardless of the initial concentrations]. Therefore, kinetics data obtained in the range 9 < pH < 13 had to be fitted to the integrated rate law for a reversible second-order system,[21]

$$\log_e \left\{ \frac{[(K-4)(C_t - C_\infty) + KQ](C_0 - C_\infty)}{[(K-4)(C_0 - C_\infty) + KQ](C_t - C_\infty)} \right\} = (k_f Q)t \tag{4a}$$

$$Q = \frac{1}{K}[A^2([B]_0 - [A]_0)^2 + 16K[A]_0[B]_0]^{1/2} \tag{4b}$$

using a weighted linear least-squares regression program for the Com-

---

(16) (a) Johnson, K. J. *Numerical Methods in Chemistry*; Marcel-Dekker: New York, 1980; Chapters 5 and 7. (b) The FORTRAN programs NONLIN, SMOOTH, and RUNGE-KUTTA of ref 16a have been translated to Microsoft BASIC for use on Commodore computers and are available on request. (c) A kinetics package comprising data acquisition, disk storage, curve fitting, plotting, printing and digital simulation for pseudo-first- and second-order reversible or irreversible systems is available in Commodore BASIC 4.0 on request.

(17) Akerlof, G. *J. Am. Chem. Soc.* **1926**, *48*, 1160.

(18) Perrin, D. D.; Dempsey, B. *Buffers For pH and Metal Ion Control*; Science Paperbacks, Chapman and Hall: London, U.K., 1974.

(19) Woodward, W. S.; Rocklin, R. D.; Murray, R. W. *Chem., Biomed. Environ. Instrum.* **1979**, *9*, 95.

(20) Roecker, L.; Kutner, W.; Gilbert, J. A.; Simmons, M. G.; Murray, R. W.; Meyer, T. J. *Inorg. Chem.* **1985**, *24*, 3784.

(21) (a) Frost, A. A.; Pearson, R. G. *Kinetics and Mechanism*, 2nd ed.; John Wiley & Sons, Inc.: New York, 1961; Chapter 8. Note that the Q term in the paper is defined differently to avoid mathematical problems from the $1/(K - 1)$ or $1/(K - 4)$ terms in this text. (b) Benson, W. W. *The Foundations of Chemical Kinetics*; McGraw-Hill: New York, 1960; Chapter 3. (c) Laidler, K. J. *Chemical Kinetics*, 2nd ed.; McGraw-Hill: New York, 1965; Chapter 1. (d) Espenson, J. H. *Chemical Kinetics and Reaction Mechanism*; McGraw-Hill: New York, 1981; Chapter 3. The unwieldy algebraic form given in this text, when corrected for missing brackets, reduces to the form used in the paper.

modore microcomputer,[16c] where C_0, C_t, and C_∞ are the concentrations of the species monitored (A or B) at times zero, t, and infinity, respectively, and K is the value of K_{com}. The calculated weighting factors,

$$W_t = \left\{\frac{(C_t - C_\infty)}{(C_0 - C_\infty)}\right\}^2 \tag{4c}$$

were applied to the data, as appropriate for the logarithmic transform, to allow the entire trace ($3 - 5t_{1/2}$) to be fitted without undue bias from data close to C_∞. The weighted second-order fits gave correlation coefficients between 0.9995 and 0.99999 despite fitting a larger segment of the curve than used for the first-order fits.

The cross reaction (eq 2) was followed at 340 nm, a maximum for $\Delta\epsilon$, after mixing equal volumes of 2×10^{-4} $[Ru^{II}(bpy)_2(py)(OH_2)]^{2+}$ and 2×10^{-5} M $[Ru^{III}(trpy)(bpy)(OH)]^{2+}$ both in H_2O/buffer solutions over the range $3 < pH < 11$ and in D_2O/NaOD solutions over the range $7 < pD < 11$ at $I = 0.005$ M (Na_2SO_4). The low electrolyte concentration was dictated by the rapidity of the reaction. The $[Ru^{III}(trpy)(bpy)(OH)]^{2+}$ solution was prepared freshly for each run by electrochemical oxidation of the Ru(II) complex. The pH was measured both before and after mixing the Ru(II) and Ru(III) solutions. Under the conditions used the extent of reaction was about 95% for $3 < pH < 8$ ($\Delta E^{\circ\prime} = 0.056$ V, $K_{eq} \simeq 9$). For pH >8, where $[Ru^{II}(trpy)(bpy)(OH_2)]^{2+}$ ($pK_a \simeq 9.7$) is deprotonated more easily than $[Ru^{II}(bpy)_2(py)(OH_2)]^{2+}$ ($pK_a = 10.8$), there is an increase in driving force for the reaction so that the extent of reaction approaches 100%. Therefore, a pseudo-first-order kinetics analysis (eq 3) was performed for the reversible second-order cross reaction. Since the decay times were rather short (20–40 ms) and the absorbance changes were small, the signal-to-noise ratio was diminished compared with the comproportionation reaction, and the fitted decay curves gave somewhat lower correlation coefficients (0.999–0.9995).

Results

Electrochemical Measurements. Cyclic voltammograms for solutions of $[Ru^{II}(bpy)_2(py)OH_2]^{2+}$ and $[Ru^{II}(trpy)(bpy)OH_2]^{2+}$ have been reported previously,[1,2,22] with both complexes displaying two reversible one-electron oxidation waves at slow sweep rates. The difference in half-wave potentials, $\Delta E_{1/2,com}$ (eq 5), is a measure of the comproportionation equilibrium constant, K_{com}, for these systems.

$$\Delta E_{1/2,com} = E_{1/2}(IV/III) - E_{1/2}(III/II) \tag{5a}$$

$$\Delta G^\circ_{com} = -nF\Delta E_{1/2,com} \tag{5b}$$

$$K_{com} = \exp(-\Delta G^\circ_{com}/RT) \tag{5c}$$

Previous studies have shown that the comproportionaion equilibrium for $[Ru^{III}(bpy)_2(py)(OH)]^{2+}$ (eq 6) is favored in the forward direction by a free energy change $\Delta G^\circ = -2.5$ kcal/mol^{-1}

$$(bpy)_2(py)Ru^{IV}{=}O^{2+} + (bpy)_2(py)Ru^{II}{-}OH_2{}^{2+} \underset{k_f}{\overset{k_r}{\rightleftharpoons}} 2(bpy)_2(py)Ru^{III}{-}OH^{2+} \tag{6}$$

($\Delta E_{1/2,com} = 0.11$ V, $K_{com} = 72$) at 25 °C over the range $2 < pH < 9$.[1] The comproportionation equilibrium for $[Ru^{III}(trpy)(bpy)(OH)]^{2+}$ (eq 7) has been reported previously to be favored

$$(trpy)(bpy)Ru^{IV}{=}O^{2+} + (trpy)(bpy)Ru^{II}{-}OH_2{}^{2+} \underset{k_f}{\overset{k_r}{\rightleftharpoons}} 2(trpy)(bpy)Ru^{III}{-}OH^{2+} \tag{7}$$

in the forward direction by a $\Delta G^\circ \simeq -3$ kcal mol^{-1} ($\Delta E_{1/2,com} = 0.13$ V, $K_{com} \simeq 200$) from cyclic voltammetry on a Au electrode[10a,11] although more recent studies by differential pulse polarography and cyclic voltammetry at carbon paste and activated glassy carbon electrodes[2a,22] have given $\Delta E_{1/2,com} \simeq 0.09$ V at neutral pH. In order to clarify this point the present work extends the investigation to include the temperature and solvent isotope dependences of these comproportionation reactions on Au electrodes under identical conditions.

$E_{1/2}$ values for the Ru(IV)/(III) and Ru(III)/(II) couples obtained in a medium of 0.10 M $LiClO_4$ + 0.01 M $HClO_4$ in both H_2O and D_2O (>99% D) from cyclic voltammetric measurements on solutions containing either $[Ru(bpy)_2(py)(OH_2)]^{2+}$ or $[Ru(trpy)(bpy)(OH_2)]^{2+}$ are summarized in Table I as a function of temperature. As noted previously, the Ru(IV)/(III) wave is only reversible at slow sweep rates (20 mV/s in H_2O, 2 mV/s in D_2O) on metal electrodes.[1] This results in the peak current for the Ru(IV)/(III) wave diminishing, relative to the Ru(III)/(II) wave, with increasing sweep rate. The sweep rate behavior of the Ru(IV)/(III) wave has been ascribed to slow heterogeneous charge transfer rates arising from the proton demands of the couple.[1,22]

Table I. $E_{1/2}$ Values vs. SSCE for the Ru(IV)/Ru(III) and Ru(III)/Ru(II) Couples of $[Ru(bpy)_2(py)(OH_2)]^{2+}$ and $[Ru(trpy)(bpy)(OH_2)]^{2+}$ in H_2O and D_2O with 0.10 M $LiClO_4$ + 0.01 M $HClO_4$[a]

T, °C	$E_{1/2}$, V		$\Delta E_{1/2,com}$, V	K_{com}
	IV/III	III/II		
$[Ru(bpy)_2(py)(OH_2)]^{2+}$ at 1.1×10^{-3} M				
5	0.83_2	0.72_3	0.109	94.4
25	0.82_8	0.72_0	0.108	66.9
25 (D_2O)[b]	0.85_7	0.75_4	0.103	55.1
$[Ru(trpy)(bpy)(OH_2)]^{2+}$ at 3×10^{-4} M				
5	0.88_3	0.76_6	0.118	137
10	0.88_2	0.76_5	0.117	121
15	0.88_3	0.76_6	0.117	111
20	0.88_1	0.76_7	0.114	91.2
25	0.88_0	0.76_7	0.113	81.3
30	0.87_7	0.76_6	0.111	70.1
25 (D_2O)[b]	0.91_1	0.79_7	0.114	84.5

[a] Au disk working electrode, Pt wire auxiliary electrode in three-compartment cell. The SSCE reference electrode = +0.236 V vs. NHE. Sweep rates were 20 mV/s in H_2O or 2–5 mV/s in D_2O. [b] Uncorrected for liquid junction potentials. Isotopic purity >99% D.

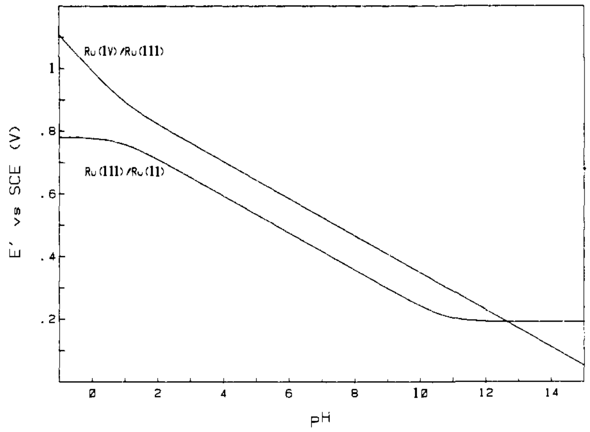

Figure 1. Calculated pH dependence of the redox potentials vs. SCE for the couples $[Ru^{IV}(bpy)_2(py)(O)]^{2+}/[Ru^{III}(bpy)_2(py)(OH)]^{2+}$ and $[Ru^{III}(bpy)_2(py)(OH)]^{2+}/[Ru^{II}(bpy)_2(py)(OH_2)]^{2+}$ at $T = 25$ °C.

The values of $\Delta E_{1/2,com}$ and K_{com} for $[Ru^{III}(bpy)_2(py)(OH)]^{2+}$ given in Table I are valid only for the range $2 < pH < 9$, where both the Ru(IV)/(III) and Ru(III)/(II) couples have been shown to vary with pH according to the Nernst equation for a one-proton/one-electron couple (−59 mV/pH).[1,20] For pH < 1 Ru(III) is present predominantly as the aqua complex, $[Ru^{III}(bpy)_2(py)(OH_2)]^{3+}$ ($pK_a = 0.85$),[1] so that the Ru(IV)/(III) couple assumes a two-proton/one-electron pH dependence (−118 mV/pH) while the Ru(III)/(II) couple becomes pH independent, leading to increasing $\Delta E_{1/2,com}$ and K_{com} values with decreasing pH. For pH >10 $[Ru^{II}(bpy)_2(py)(OH_2)]^{2+}$ ($pK_a = 10.8$)[1] is deprotonated to form the hydroxo complex. Electrochemical measurements for this pH range have shown that the Ru(III)/(II) couple becomes independent of pH while the Ru(IV)/(III) couple continues to decrease with increasing pH, leading to decreasing values of $\Delta E_{1/2,com}$ and K_{com} with increasing pH.[20] The pH dependence of these redox couples (Figure 1) can be calculated from eq 8 and 9 with use of the formal reduction potentials, $E^{\circ\prime}_{IV/III} = +0.99$ V and $E^{\circ\prime}_{III/II} = +0.78$ V vs. SCE, determined previ-

---

(22) Cabaniss, G. E.; Diamantis, A. A.; Murphy, W. R.; Linton, R. W.; Meyer, T. J. *J. Am. Chem. Soc.* **1985**, *107*, 1845.

(23) Nakamoto, K. *Infrared and Raman Spectra of Inorganic and Coordination Compounds*, 3rd ed.; Wiley-Interscience: New York, 1978.

ously,[1] where $E_{\mathrm{IV/III}}$ and $E_{\mathrm{III/II}}$ are the calculated potentials and

$$E_{\mathrm{IV/III}} = E^{\circ\prime}_{\mathrm{IV/III}} - 0.05916[\mathrm{pH} - \log (K_a^{\mathrm{III}} + [\mathrm{H}^+])] \quad (8)$$

$$E_{\mathrm{III/II}} = E^{\circ\prime}_{\mathrm{III/II}} - 0.05916[\log (K_a^{\mathrm{III}} + [\mathrm{H}^+]) - \log (K_a^{\mathrm{II}} + [\mathrm{H}^+])] \quad (9)$$

K_a^{II} and K_a^{III} are the acid dissociation constants for the Ru(II) and Ru(III) aqua complexes, respectively. When the pK_a values above are used, the redox potentials at pH 7 are calculated to be $E_{1/2} = +0.526$ V for Ru(IV)/(III) and $E_{1/2} = +0.416$ V for Ru(III)/(II). Similarly, the point at which the two couples intersect ($\Delta G^\circ = 0$, $K_{\mathrm{com}} = 1$) is calculated to be at pH 12.6. Thus, for pH >13 the comproportionation (eq 6) is nonspontaneous in the forward direction.

For solutions of $[\mathrm{Ru^{II}(trpy)(bpy)(OH_2)}]^{2+}$ measurements of $E_{1/2}$ vs. pH have been reported recently for the entire range 0 < pH < 13 with use of activated glassy carbon and carbon paste electrodes.[2a] The pH dependence of the Ru(IV)/(III) and Ru(III)/(II) couples followed the same trends as described above for $[\mathrm{Ru^{II}(bpy)_2(py)(OH_2)}]^{2+}$. From their extensive data Takeuchi et al.[2a] were able to estimate pK_a values for the aqua complexes; $[\mathrm{Ru^{III}(trpy)(bpy)(OH_2)}]^{3+}$ (p$K_a \simeq 1.7$) and $[\mathrm{Ru^{II}(trpy)(bpy)(OH_2)}]^{2+}$ (p$K_a \simeq 9.7$). The values of $E_{1/2}$, $\Delta E_{1/2,\mathrm{com}}$, and K_{com} at pH 2 given in Table I were therefore obtained with a mixture of the Ru(III) aqua and hydroxo complexes present. However, when eq 8 and 9 with the estimated pK_a values above were used, the redox potentials at pH 7 are calculated to be $E_{1/2} = +0.573$ V for Ru(IV)/Ru(III) and $E_{1/2} = +0.482$ V for Ru(III)/Ru(II). These values give the corrected value of $\Delta E_{1/2,\mathrm{com}} = 0.091$ V ($K_{\mathrm{com}} = 35$, $\Delta G^\circ = -2.1$ kcal mol^{-1}) appropriate for pH 7 at 25 °C, in agreement with the value of $\simeq 0.09$ V (3 < pH < 9) reported previously.[2a] For pH >10 the driving force for the comproportionation was found to decrease with increasing pH until $\Delta E_{1/2,\mathrm{com}} = 0$ V at pH $\simeq$ 11.5. For pH >11.5 only a single wave was observed, decreasing at 30 mV/pH as expected for a one-proton/two-electron couple.[2a] These observations are consistent with the Ru(IV)/(III) couple crossing the Ru(III)/(II) couple at pH $\simeq$ 11.5 so that for pH >12 $[\mathrm{Ru^{III}(trpy)(bpy)(OH)}]^{2+}$ becomes unstable with respect to disproportionation.

Kinetics Measurements. The kinetics of the comproportionation reaction (eq 1) between $[\mathrm{Ru^{II}(bpy)_2(py)(OH_2)}]^{2+}$ and $[\mathrm{Ru^{IV}(bpy)_2(py)(O)}]^{2+}$ have been reported in a previous communication to be first order with respect to both reactants.[14] This reaction was investigated at 25 °C within the range 2 < pH < 13 for an ionic strength of 0.10 M ($\mathrm{Na_2SO_4}$) in both $\mathrm{H_2O}$ and $\mathrm{D_2O}$, and the results are summarized in Table II. The pH range of the investigation was limited at high pH by the fact that the reaction becomes pH dependent above the pK_a for $[\mathrm{Ru^{II}(bpy)_2(py)(OH_2)}]^{2+}$

$$\mathrm{H_2O} + [\mathrm{Ru^{IV}(bpy)_2(py)(O)}]^{2+} + [\mathrm{Ru^{II}(bpy)_2(py)(OH)}]^{+} \rightarrow \mathrm{OH^-} + 2[\mathrm{Ru^{III}(bpy)_2(py)(OH)}]^{2+}$$

for which $\Delta G^\circ = 0$ at pH $\simeq$ 12.6 so that the reaction between Ru(IV) and Ru(II) becomes nonspontaneous for pH >13, since Ru(III) is unstable with respect to disproportionation. This situation arises from the difference in pH dependence between the Ru(IV)/(III) couple

$$[\mathrm{Ru^{IV}(bpy)_2(py)(O)}]^{2+} + \mathrm{H_2O} + \mathrm{e} \rightarrow [\mathrm{Ru^{III}(bpy)_2(bpy)(OH)}]^{2+} + \mathrm{OH^-}$$

and the Ru(III)/(II) couple

$$[\mathrm{Ru^{III}(bpy)_2(py)(OH)}]^{2+} + \mathrm{e} \rightarrow [\mathrm{Ru^{II}(bpy)_2(py)(OH)}]^{+}$$

A further experimental complication arises from the instability of Ru(IV)=O and Ru(III)—OH for pH > 12,[20] but the ligand-based decomposition reactions are relatively slow and had no effect on the results reported here.

Under the pseudo-first-order conditions used for the kinetics measurements the comproportionation reaction was driven to >99% completion at neutral pH but only to 73% completion at pH 12.7, so that the observed rate constant becomes faster than k_f in basic media. Obtaining k_f by using the full second-order kinetics analysis requires independent knowledge of the comproportionation equilibrium constant, K_{com}, which can be calculated from the pH dependence of the redox couples (eq 8 and 9) provided that the pK_a of $[\mathrm{Ru^{II}(bpy)_2(py)(OH_2)}]^{2+}$ is well determined. Since this pK_a was previously measured at far higher ionic strength than used for the kinetics studies, the value was redetermined by spectrophotometric titration with NaOH (Figure 2) at an ionic strength of 0.10 M ($\mathrm{Na_2SO_4}$).

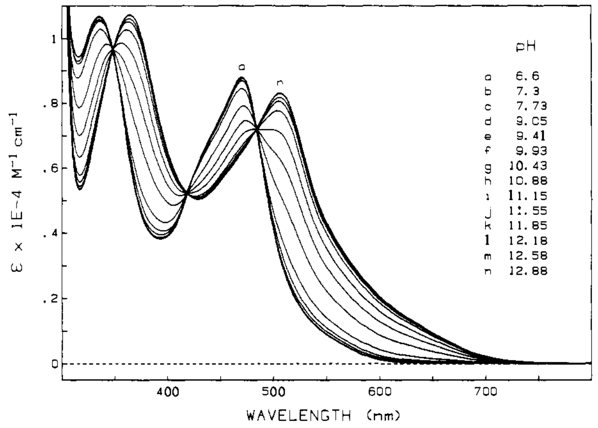

Figure 2. Spectrophotometric titration of $[\mathrm{Ru^{II}(bpy)_2(py)(OH_2)}]^{2+}$ ($\lambda_{\mathrm{max}} = 335.5$, 470 nm) with NaOH solution for 7 < pH < 13 at $I = 0.10$ M ($\mathrm{Na_2SO_4}$), $T = 22$ °C.

Table II. pOH or pOD Dependence of the Comproportionation Reaction between $[\mathrm{Ru^{IV}(bpy)_2(py)(O)}]^{2+}$ and $[\mathrm{Ru^{II}(bpy)_2(py)(OH_2)}]^{2+}$ at 25 °C with $I = 0.10$ M ($\mathrm{Na_2SO_4}$)

pOH	pOD	N^a	$K_{\mathrm{com}}{}^b$	$k_f \times 10^{-5}$,^{c} M^{-1} s^{-1}
11.39		7	75.2	2.179 ± 0.019
7.85		11	70.7	2.179 ± 0.032
4.57		12	67.8	2.066 ± 0.042
3.81		10	50.7	1.841 ± 0.013
3.56		9	49.1	1.469 ± 0.011
2.66		11	15.7	0.698 ± 0.008
2.36		11	9.01	0.472 ± 0.005
1.74		11	2.39	0.317 ± 0.003
1.67		7	2.02	0.293 ± 0.004
1.28		8	0.85	0.258 ± 0.003
1.29		9	0.85	0.252 ± 0.003
	7.00	10	70.7	0.135 ± 0.001
	4.12	8	63.1	0.142 ± 0.001
	3.12	7	32.1	0.160 ± 0.001
	2.12	9	5.43	0.164 ± 0.001
	1.12	8	0.58	0.166 ± 0.002

[a] N = number of replicates averaged. [b] Values calculated based on eq 8 and 9 with pK_b = 3.2. [c] Error bars are for one standard deviation of the mean.

The smoothed values of absorbance vs. $\mathrm{pH_{meas}}$ at four wavelengths were fitted to eq 10a by nonlinear least-squares regression, yielding an average value of pK_a = 10.68 ± 0.005 (average standard deviation = ±0.04), which is close to the value of 10.79

$$A_\lambda = [\mathrm{Ru}]_{\mathrm{total}}\left\{\frac{\epsilon_{\lambda(\mathrm{HA})}}{1 + 10^{(\mathrm{pH}-\mathrm{p}K_a)}} + \frac{\epsilon_{\lambda(\mathrm{A})}}{1 + 10^{(\mathrm{p}K_a-\mathrm{pH})}}\right\} \quad (10a)$$

determined previously at $I = 1.0$ M ($\mathrm{Na_2SO_4}$).[1] However, the more meaningful pK_b value was obtained by fitting the absorbance data vs. the calibrated pOH measurements to eq 10b, yielding an average value of pK_b = 3.20 ± 0.004 (average standard deviation = ±0.05), which is somewhat higher than the value of 2.94 obtained at $I = 1.0$ M ($\mathrm{Na_2SO_4}$).[1] The rate constants, k_f, for

$$A_\lambda = [\mathrm{Ru}]_{\mathrm{total}}\left\{\frac{\epsilon_{\lambda(\mathrm{HA})}}{1 + 10^{(\mathrm{p}K_b-\mathrm{pOH})}} + \frac{\epsilon_{\lambda(\mathrm{A})}}{1 + 10^{(\mathrm{pOH}-\mathrm{p}K_b)}}\right\} \quad (10b)$$

the comproportionation reaction (Table II) were obtained by the second-order analysis (see above) with K_{com} values calculated from the pOH dependence of the redox potentials and pK_b = 3.20 to

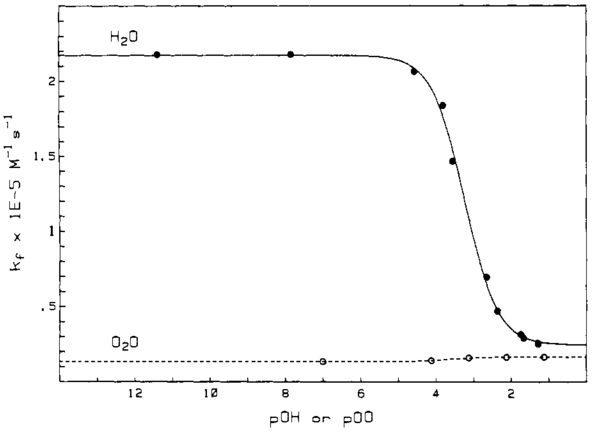

Figure 3. pOH dependence (●) or pOD dependence (○) of the forward rate constant for the comproportionation reaction between $[Ru^{IV}(bpy)_2(py)(O)]^{2+}$ and $[Ru^{II}(bpy)_2(py)(OH_2)]^{2+}$ at $I = 0.10$ M (Na_2SO_4), $T = 25$ °C.

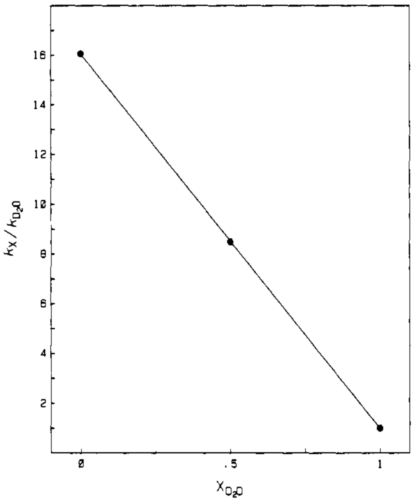

Figure 4. Dependence of the rate constant for the comproportionation reaction between $[Ru^{IV}(bpy)_2(py)(O)]^{2+}$ and $[Ru^{II}(bpy)_2(py)(OH_2)]^{2+}$ on solvent mole fraction of deuterium (X) without added electrolyte, $I = 3.3 \times 10^{-4}$ M, $T = 25$ °C.

Table III. Temperature and Solvent Isotope Dependence for the Comproportionation Reaction between $[Ru^{IV}(bpy)_2(py)(O)]^{2+}$ and $[Ru^{II}(bpy)_2(py)(OH_2)]^{2+}$ in H_2O, HDO ($X = 0.5$), and D_2O with $I = 3.3 \times 10^{-4}$ M at pH or pD = 7

solvent	T, °C	N^a	$k' \times 10^{-4}$,[b] $M^{-1}\,s^{-1}$
H_2O	5.0	11	2.95 ± 0.10
	15.0	16	3.70 ± 0.05
	20.0	15	3.93 ± 0.03
	25.3	17	4.46 ± 0.03
	30.0	13	4.77 ± 0.05
	35.0	12	5.21 ± 0.04
	45.0	16	5.92 ± 0.03
	55.0	6	6.60 ± 0.03
HDO[c]	25.3	18	2.355 ± 0.015
D_2O	6.0	7	0.174 ± 0.003
	15.1	16	0.221 ± 0.004
	25.3	15	0.278 ± 0.002
	35.0	14	0.358 ± 0.007
	45.0	11	0.468 ± 0.012

[a] N = number of replicates averaged. [b] Error bars are for one standard deviation of the mean. [c] $X = 0.5$, mole fraction of deuterium in a H_2O:D_2O mixture.

obtain $\Delta E_{1/2,\text{com}}$ and hence K_{com}. The rate constants in D_2O solution were corrected by assuming the same value for pK_b since the absorbance vs. pOD behavior was very similar to that in H_2O.

The most striking feature of these results is the unusually large solvent isotope effect on the rate constant, with $[k_{H_2O}/k_{D_2O}] = 16.1 \pm 0.4$ over a broad pH/pOH range at 25 °C, as shown in Figure 3. In the absence of supporting electrolyte ($I = 3.3 \times 10^{-4}$ M), where $k_{H_2O} = (4.45 \pm 0.03) \times 10^4$ $M^{-1}\,s^{-1}$ at 25.3 °C, the solvent isotope effect is identical, with $[k_{H_2O}/k_{D_2O}] = 16.1 \pm 0.2$ (Table III). Since the electrochemical measurements show that there is no significant difference in $\Delta G°_{\text{com}}$ between H_2O and D_2O it follows that the large isotope effect is kinetic in origin. The kinetic isotope effect for pOH $\simeq$ 7 displays a linear dependence on the mole fraction of deuterium in the solvent, as shown in Figure 4.

The pOH dependence of the forward rate constant in H_2O was fitted to a model (eq 11) involving two forms of Ru(II), $[Ru^{II}(bpy)_2(py)(OH_2)]^{2+}$ being the dominant form for pH <10 and $[Ru^{II}(bpy)_2(py)(OH)]^+$ predominating for pH >11, each reacting with $[Ru^{IV}(bpy)_2(py)(O)]^{2+}$ to yield the Ru(III) hydroxo complex.

$$k_f = \frac{k_{OH} + k_{H_2O}K_b/[OH^-]}{1 + K_b/[OH^-]} \tag{11a}$$

$$k_f = \frac{k_{OH} + k_{H_2O}10^{(pOH-pK_b)}}{1 + 10^{(pOH-pK_b)}} \tag{11b}$$

Since the well-determined quantity was pOH in most of our measurements, eq 11b was used to fit the data by nonlinear least-squares regression, yielding values of pK_b = 3.23 ± 0.10, $k_{H_2O} = (2.174 \pm 0.028) \times 10^5$ $M^{-1}\,s^{-1}$, and $k_{OH} = (0.247 \pm 0.024) \times 10^5$ $M^{-1}\,s^{-1}$. The fit is shown as the solid curve in Figure 3. The value of pK_b obtained from the kinetics agrees very well with the value of 3.20 ± 0.05 determined spectrophotometrically.

The comproportionation reaction in D_2O shows little dependence on pOD in the region of the pK_b (Figure 3). The data were fitted to eq 11b with the value of k_{D_2O} held fixed, resulting in fitted values of pK_b = 3.66 ± 0.21, and $k_{OD} = (0.165 \pm 0.001) \times 10^5$ $M^{-1}\,s^{-1}$. This fit is shown as the dashed curve in Figure 3. Refitting the experimental data by using the fitted value for pK_b results in the corrected rate constant passing through a maximum near the pK_b and decreasing rapidly for lower pOD values. This seems to indicate that the pK_b in D_2O is actually much closer to the value of 3.20 measured in H_2O and that the fitted value is subject to a large uncertainty due to the very small change in rate constant with pOD.

The temperature dependences of the rate constants for the pH independent pathway, in the absence of supporting electrolyte, are summarized in Table III. These data give quite linear plots of $\log_e$ (k'/T) vs. ($1/T$), as shown in Figure 5, or $\log_e$ (k') vs. ($1/T$), yielding, from linear least-squares fits, the activation parameters in Table VI.

The kinetics of the cross reaction (eq 2) between $[Ru^{II}(bpy)_2(py)(OH_2)]^{2+}$ and $[Ru^{III}(trpy)(bpy)(OH)]^{2+}$, which is favored in the forward direction by a driving force $\Delta E°' = 0.056$ V ($\Delta G° = -1.3$ kcal mol^{-1}, $K_{\text{com}} \simeq 9$) at neutral pH, were investigated at 25 °C within the range 3 < pOH < 11 for an ionic strength of 0.005 M in both H_2O and D_2O, and the data are summarized in Table IV. Although less striking than for the comproportionation reaction, a solvent kinetic isotope effect of $[k_{H_2O}/k_{D_2O}] = 5.8 \pm 0.4$ exists for pOH > 5, as shown in Figure 6. Within experimental error the cross reaction also displays a linear dependence on the mole fraction of deuterium in the solvent (Figure 7). These are remarkable observations for such a simple M(III)/M(II) electron transfer reaction. Furthermore, unlike the comproportionation reaction there is a dramatic *increase* in the rate constant in the vicinity of the pK_a of $[Ru^{II}(bpy)_2(py)(OH_2)]^{2+}$, where the "pseudo-self-exchange" reaction

$$Ru^{II}(bpy)_2(py)(OH)^+ + Ru^{III}(trpy)(bpy)(OH)^{2+} \rightarrow Ru^{III}(bpy)_2(py)(OH)^{2+} + Ru^{II}(trpy)(bpy)(OH)^+$$

is accessible. With use of the value of pK_b = 3.20 for $[Ru^{II}(bpy)_2(py)(OH)]^+$, the observed values of k' vs. pOH were fitted by nonlinear least-squares regression to eq 11b, yielding values of $k_{H_2O} = (4.0 \pm 0.4) \times 10^5$ $M^{-1}\,s^{-1}$ and $k_{OH} = (4.4 \pm 0.3) \times 10^7$ $M^{-1}\,s^{-1}$. Similar extrapolations from the limited data in D_2O give a value of $k_{OD} \simeq 2.9 \times 10^7$ $M^{-1}\,s^{-1}$.

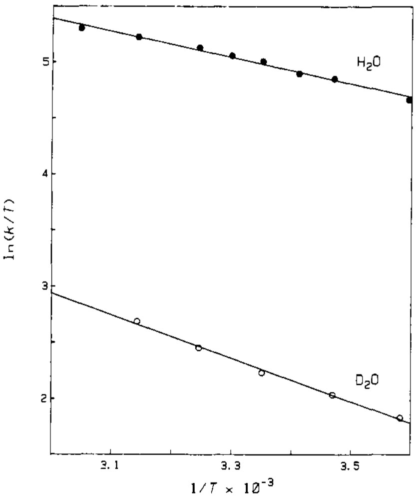

Figure 5. Temperature dependence of the rate constant for the comproportionation reaction between $[Ru^{IV}(bpy)_2(py)(O)]^{2+}$ and $[Ru^{II}(bpy)_2(py)(OH_2)]^{2+}$ in H_2O (●) and D_2O (○) without added electrolyte, $I = 3.3 \times 10^{-4}$ M.

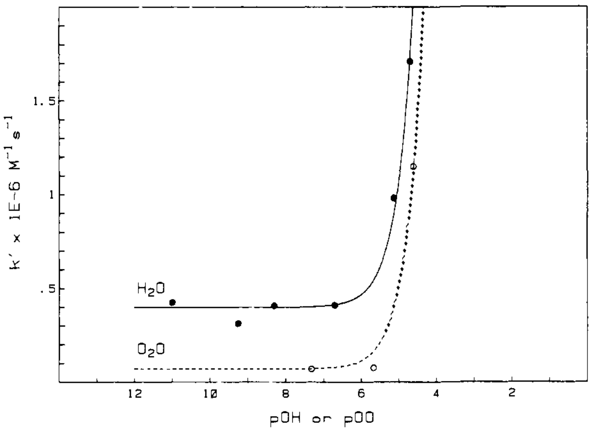

Figure 6. pOH dependence (●) or pOD dependence (○) of the rate constant for the cross reaction between $[Ru^{III}(trpy)(bpy)(OH)]^{2+}$ and $[Ru^{II}(bpy)_2(py)(OH_2)]^{2+}$ at $I = 0.005$ M (Na_2SO_4), $T = 25$ °C.

Table IV. pOH or pOD Dependence for the Cross Reaction between $[Ru^{III}(trpy)(bpy)(OH)]^{2+}$ and $[Ru^{II}(bpy)_2(py)(OH_2)]^{2+}$ at 25 °C with $I = 0.005$ M (Na_2SO_4)

pOH	pOD	N^a	$k' \times 10^{-5}$,[b] $M^{-1}\ s^{-1}$
10.99		19	4.26 ± 0.18
9.25		19	3.13 ± 0.10
8.30		13	4.08 ± 0.21
6.70		20	4.10 ± 0.12
5.14		13	9.82 ± 0.54
4.70		7	17.1 ± 0.37
3.00			c
	7.32	14	0.706 ± 0.014
	5.67	12	0.780 ± 0.011
	4.61	14	11.5 ± 0.9
	3.00		c

[a] N = number of replicates averaged. [b] Error bars are for one standard deviation of the mean. [c] Too fast to measure.

The temperature dependence of the rate constants for the pH independent pathway of the cross reaction ($I = 0.005$ M) are summarized in Table V. The data give reasonably linear plots of $\log_e (k'/T)$ vs. $(1/T)$, as shown in Figure 8, or $\log_e (k')$ vs. $(1/T)$, yielding the activation parameters in Table VI. As for the comproportionation reaction, the rate difference between H_2O and D_2O solution appears in the activation enthalpy, a feature that will be discussed below.

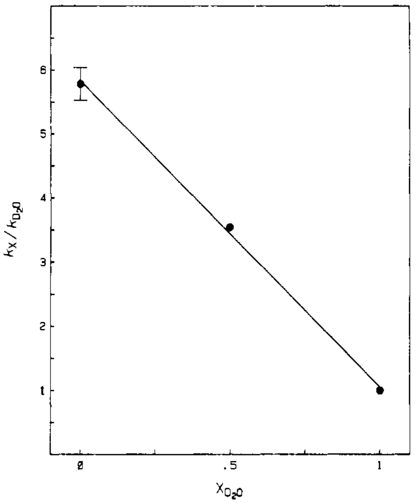

Figure 7. Dependence of the rate constant for the cross reaction between $[Ru^{III}(trpy)(bpy)(OH)]^{2+}$ and $[Ru^{II}(bpy)_2(py)(OH_2)]^{2+}$ on solvent mole fraction of deuterium (X) at $I = 0.005$ M (Na_2SO_4), $T = 25$ °C.

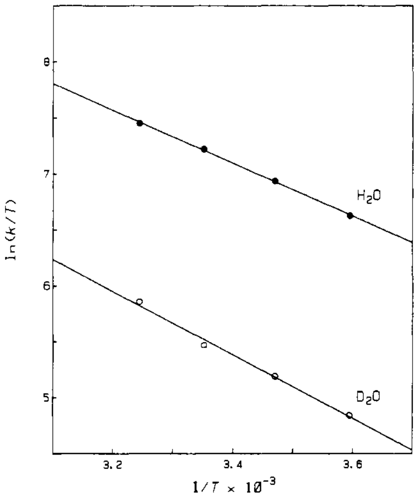

Figure 8. Temperature dependence of the rate constant for the cross reaction between $[Ru^{III}(trpy)(bpy)(OH)]^{2+}$ and $[Ru^{II}(bpy)_2(py)(OH_2)]^{2+}$ in H_2O (●) and D_2O (○) at $I = 0.005$ M (Na_2SO_4).

Table V. Temperature and Solvent Isotope Dependence for the Cross Reaction between $[Ru^{III}(trpy)(bpy)(OH)]^{2+}$ and $[Ru^{II}(bpy)_2(py)(OH_2)]^{2+}$ in H_2O, HDO ($X = 0.5$), and D_2O with $I = 0.005$ M (Na_2SO_4) at pH or pD ≃ 7

solvent	T, °C	N^a	$k' \times 10^{-5}$,[b] $M^{-1}\ s^{-1}$
H_2O	5.0	14	2.10 ± 0.02
	15.0	13	2.97 ± 0.08
	25.2	13	4.08 ± 0.21
	35.0	12	5.31 ± 0.18
HDO[c]	25.2	18	2.50 ± 0.04
D_2O	5.0	13	0.352 ± 0.005
	15.0	18	0.518 ± 0.007
	25.2	14	0.706 ± 0.014
	35.0	4	1.080 ± 0.020

[a] N = number of replicates averaged. [b] Error bars are for one standard deviation of the mean. [c] $X = 0.5$, mole fraction of deuterium in a H_2O:D_2O mixture.

Discussion

The Comproportionation Reaction. From the pH dependence of the kinetics study (Figure 3), comproportionation between $Ru^{IV}{=}O^{2+}$ and $Ru^{II}{-}OH_2^{2+}$ occurs by two well defined pathways which differ in the proton content at Ru(II). The first pathway (eq 12), which is dominant in the range 2 < pH < 10, involves the Ru(II) aqua complex. In the second pathway (eq 13), which

$$(bpy)_2(py)Ru^{IV}{=}O^{2+} + (bpy)_2(py)Ru^{II}{-}OH_2^{2+} \xrightarrow{k_{H_2O}} 2(bpy)_2(py)Ru^{III}{-}OH^{2+} \quad (12)$$

is favored for pH >11, the Ru(II) hydroxo complex is the re-

Table VI. Summary of Thermodynamic and Kinetic Data for the Comproportionation and Cross Reactions at pH or pD $\simeq$ 7[a]

medium	$k^{25\,°C} \times 10^{-4}$, $M^{-1}\,s^{-1}$	$\Delta H^{\ddagger}$, kcal mol^{-1} [E_a], kcal mol^{-1}	$\Delta S^{\ddagger}$, cal K^{-1} mol^{-1} [A], s^{-1}	$\Delta G°$, kcal mol^{-1}
Reaction 1: $(bpy)_2(py)Ru^{IV}{=}O^{2+} + (bpy)_2(py)Ru^{II}{-}OH_2^{2+}$				
H_2O[b]	4.46 ± 0.03	2.33 ± 0.13 [2.93 ± 0.10]	−29.5 ± 0.4 [6.1 ± 1.1] × 10^6	−2.5
D_2O[b]	0.278 ± 0.003	3.86 ± 0.23 [4.43 ± 0.15]	−29.8 ± 0.8 [5.0 ± 1.5] × 10^6	−2.4
Reaction 2: $(trpy)(bpy)Ru^{III}{-}OH^{2+} + (bpy)_2(py)Ru^{II}{-}OH^{2+}$				
H_2O[c]	40.8 ± 2.1	4.70 ± 0.11 [5.28 ± 0.09]	−17.1 ± 0.4 [3.0 ± 0.5] × 10^9	−1.3
D_2O[c]	7.06 ± 0.14	5.65 ± 0.36 [6.23 ± 0.36]	−17.3 ± 1.2 [2.7 ± 1.3] × 10^9	−1.2[d]

[a] Error bars are for one standard deviation. [b] $I = 3.3 \times 10^{-4}$ M (no added electrolyte). [c] $I = 0.005$ M (Na_2SO_4). [d] Assuming $pK_a(D_2O) \simeq pK_a(H_2O) = 1.7$ for $[Ru^{III}(trpy)(bpy)(OH_2)]^{3+}$, $\Delta E°' = 0.056$ V (H_2O); $\Delta E°' = 0.054$ V (D_2O) at pH 7.

ductant and consequently the overall reaction must involve net H^+ transfer from solvent. In comparing the two pathways there

$$(bpy)_2(py)Ru^{IV}{=}O^{2+} + (bpy)_2(py)Ru^{II}{-}OH^{+} + H_2O \xrightarrow{k_{OH}} 2(bpy)_2(py)Ru^{III}{-}OH^{2+} + OH^{-} \quad (13)$$

are two striking observations. The first is the considerable decrease in reactivity for the Ru(II) hydroxo complex with $[k_{H_2O}/k_{OH}]^{25\,°C} = 8.8$. The second is the dramatic difference in the H_2O/D_2O kinetic isotope effects for the two pathways with $[k_{H_2O}/k_{D_2O}]^{25\,°C} = 16.1$ and $[k_{OH}/k_{OD}]^{25\,°C} = 1.5$.

There are some unusual features associated with the k_{H_2O} pathway in addition to the dramatic H_2O/D_2O kinetic isotope effect. Compared with self-exchange rates for related reactions like $[Ru(bpy)_2(py)(Cl)]^{2+/+}$ or $[Ru(bpy)_3]^{3+/2+}$, the value of k_{H_2O} is surprisingly slow especially given its favorable driving force, $\Delta G° = -2.5$ kcal mol^{-1}.[24-26] The mechanism involved *cannot* be via an initial outer-sphere electron transfer

$$(bpy)_2(py)Ru^{IV}{=}O^{2+} + (bpy)_2(py)Ru^{II}{-}OH_2^{2+} \rightarrow (bpy)_2(py)Ru^{III}{-}O^{+} + (bpy)_2(py)Ru^{III}{-}OH_2^{3+} \quad (14a)$$

followed by rapid proton transfer

$$(bpy)_2(py)Ru^{III}{-}O^{+} + (bpy)_2(py)Ru^{III}{-}OH_2^{3+} \xrightarrow{\text{rapid}} 2(bpy)_2(py)Ru^{III}{-}OH^{2+} \quad (14b)$$

In addition to the normal activational requirements, an initial outer-sphere electron-transfer step (eq 14a) involves the free energy cost, $\Delta G°'_{os}$, associated with the formation of the products, Ru(III)-OH_2^{3+} and Ru(III)-O^+, which are thermodynamically disfavored because of their nonequilibrium proton distributions. The free energy change for the initial step (eq 14a) can be calculated from

$$\Delta G°'_{os} = \Delta G°'_{ion} + \Delta G°'_{rxn} \quad (15a)$$

$$\Delta G°'_{ion} = -RT \log_e \left\{\frac{K_{a2}}{K_{a1}}\right\} \quad (15b)$$

where $\Delta G°'_{rxn}$ is the free energy change for the overall reaction (−2.5 kcal mol^{-1}) and K_{a1} and K_{a2} are the first and second proton ionization constants for $[Ru^{III}(bpy)_2(py)(OH_2)]^{3+}$. By using the values $pK_{a1} = 0.85$[1] and $pK_{a2} \geq 12$[27] the initial free energy change for outer-sphere electron transfer is calculated to be $\Delta G°'_{os} \geq 12.7$ kcal mol^{-1}. Thus, the *minimum* free energy of activation for an initial outer-sphere electron-transfer step is $\Delta G^{\ddagger}_{os} = \Delta G°'_{os}$ and the *maximum* rate constant can be calculated from the expression

$$k = (\nu_{et}K_A)\exp(-\Delta G^{\ddagger}_{os}/RT) \quad (16)$$

where K_A is the preassociation equilibrium constant for the reactants and ν_{et} is the frequency factor for electron transfer.[26] Using a value of $\nu_{et}K_A \simeq [k_BT/h] = 6.2 \times 10^{12}$ s^{-1} gives $k \leq 3 \times 10^3$ M^{-1} s^{-1} at 25 °C, which is considerably less than the experimentally observed value of $k_{H_2O} = 2.18 \times 10^5$ M^{-1} s^{-1} or $k_{D_2O} = 1.35 \times 10^4$ M^{-1} s^{-1} ($I = 0.10$ M) but close to the value observed in D_2O without added electrolyte, where $k_{D_2O} = 2.78 \times 10^3$ M^{-1} s^{-1} at 25 °C. In fact, if just the activational requirement expected for an outer-sphere reaction arising from solvent dipole reorientation were included,[26] the calculated maximum rate constant would be *considerably less* than the value above.

From the magnitude of the kinetic isotope effect it is evident that in the redox step associated with the k_{H_2O} pathway (Figure 3) there is considerable proton, as well as electron, transfer character. The linear dependence of k_{H_2O} on mole fraction of added deuterium (Figure 4) reveals that the H/D isotopic fractionation factor for the bound H_2O molecule in $[Ru(bpy)_2(py)(OH_2)]^{2+}$ is close to unity, comparable to bulk water, and further that, to any significant degree, only a single proton is involved in the proton coupled redox step.[28]

Although mechanistically complex, as shown by the large H/D kinetic isotope effect, there is a clear thermodynamic advantage for the direct proton coupled electron transfer pathway in reaction 12. The initial products of the reaction, $[Ru^{III}(bpy)_2(py)(OH)]^{2+}$, are formed with the proton composition appropriate to the pH of the medium, avoiding the "high energy" intermediates, $[Ru^{III}(bpy)_2(py)(OH_2)]^{3+}$ and $[Ru^{III}(bpy)_2(py)(O)]^{+}$, required by an outer-sphere electron transfer pathway.

Above pH 10.8, where $[Ru^{II}(bpy)_2(py)(OH)]^{+}$ is the dominant form of Ru(II), the proton coupled pathway (eq 12) becomes thermodynamically disfavored with increasing pH, due to the decreasing equilibrium concentration of the Ru(II) aqua ion. Eventually, a second pathway (eq 17a,b) involving $[Ru^{II}(bpy)_2(py)(OH)]^{+}$ as the reductant appears for which electron transfer to Ru(IV) is the rate-determining step.

$$(bpy)_2(py)Ru^{IV}{=}O^{2+} + (bpy)_2(py)Ru^{II}{-}OH^{+} \xrightarrow{k_{OH}} (bpy)_2(py)Ru^{III}{-}O^{+} + (bpy)_2(py)Ru^{III}{-}OH^{2+} \quad (17a)$$

$$(bpy)_2(py)Ru^{III}{-}O^{+} + H_2O \xrightarrow{\text{rapid}} (bpy)_2(py)Ru^{III}{-}OH^{2+} + OH^{-} \quad (17b)$$

Since there is no thermodynamic advantage for a proton coupled redox step in the alternative pathway involving the Ru(II) hydroxo ion, there is a *dramatic increase* in the H_2O/D_2O kinetic isotope effect for pH >10 to a final value consistent with expectations for a typical outer-sphere electron transfer.[29] Indeed, there is no reason to believe that the reaction does not proceed via an initial outer-sphere electron transfer (eq 17a) followed by a rapid H^+ transfer from solvent (eq 17b). However, the rate constant $k_{OH} = 2.47 \times 10^4$ M^{-1} s^{-1} is still well below that expected for a *simple* outer-sphere reaction. For example, in the cross reaction between $[Ru^{III}(trpy)(bpy)(OH)]^{2+}$ and $[Ru^{II}(bpy)_2(py)(OH)]^{+}$, where there are no proton transfer restrictions on an initial outer-sphere electron transfer step, $k(25\ °C) = (4.4 \pm 0.3) \times 10^7$ M^{-1} s^{-1}. However, for the k_{OH} pathway there is an additional free energy cost arising from the appearance of Ru^{III}-O^+ as a product. At a pH value sufficiently high that pH $\simeq pK_{a2}$ for $[Ru^{III}(bpy)_2(py)(OH_2)]^{3+}$, the Ru(III) products in reaction 17a would be formed in their equilibrium proton compositions. The fact that k_{OH} is relatively slow suggests that $pK_{a2} \gg 12$ for the Ru(III) complex.[27]

---

[24] Callahan, R. W.; Keene, F. R.; Meyer, T. J.; Salmon, D. J. *J. Am. Chem. Soc.* **1977**, *99*, 1064.

[25] Chan, M. S.; Wahl, A. C. *J. Phys. Chem.* **1978**, *82*, 2542.

[26] (a) Sutin, N. *Acc. Chem. Res.* **1982**, *15*, 275. (b) Sutin, N. *Prog. Inorg. Chem.* **1983**, *30*, 441.

[27] The pK_a or $[Ru^{III}(bpy)_2(py)(OH)]^{2+}$ has not been determined directly. However, the results of electrochemical measurements up to pH 13 for both this complex and $[Ru^{III}(trpy)(bpy)(OH)]^{2+}$ show that $pK_{a2} > 13$.

[28] Albery, W. J. *Proton Transfer Reactions*; Caldin, E., Gold, V., Eds.; Wiley-Interscience: New York, 1975; Chapter 9.

[29] (a) Guarr, T.; Buhks, E.; McLendon, G. *J. Am. Chem. Soc.* **1983**, *105*, 3263. (b) Yee, E. L.; Cave, R. J.; Guyer, K. L.; Tyma, P. D.; Weaver, M. J. *J. Am. Chem. Soc.* **1979**, *101*, 1131.

Scheme II

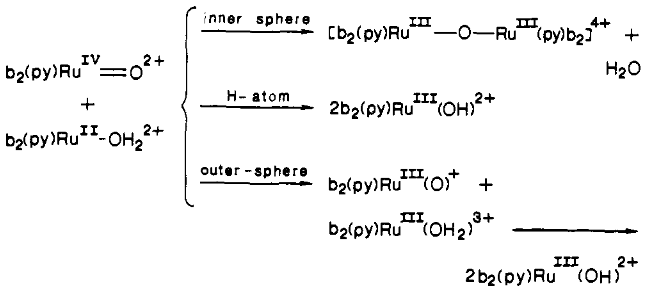

Details of the Comproportionation Mechanism. In principle, there are a series of accessible pathways for the reaction between $[Ru^{IV}(bpy)_2(py)(O)]^{2+}$ and $[Ru^{II}(bpy)_2(py)(OH_2)]^{2+}$; three of the more likely are shown in Scheme II. The inner-sphere pathway, which involves displacement of H_2O from $[Ru^{II}(bpy)_2(py)(OH_2)]^{2+}$ and oxo-bridge formation, is potentially of significant synthetic value for the preparation of oxo-bridged dimers but is apparently too slow to play an important role in aqueous solution. The μ-oxo-bis(pyridyl) dimer is a known compound, but it has been prepared by displacement of H_2O in the corresponding diaqua dimer and not by reaction between Ru(II) and Ru(IV).[8c] An inner-sphere mechanism has been proposed to account for the oxidation of $[Ru^{II}(NH_3)_5(S)]^{2+}$ (S = acetone) by ClO_4^- or O_2 in acetone solution via steps like[30]

$$Ru(NH_3)_5(S)^{2+} + ClO_4^- \rightleftharpoons Ru(NH_3)_5(O\text{-}ClO_3)^+ + S$$

$$Ru(NH_3)_5(O\text{-}ClO_3)^+ \rightarrow Ru^{IV}(NH_3)_5(O)^{2+} + ClO_3^-$$

$$Ru^{IV}(NH_3)_5(O)^{2+} + Ru^{II}(NH_3)_5(S)^{2+} \rightarrow (NH_3)_5Ru^{III}\text{-}O\text{-}Ru^{III}(NH_3)_5^{4+}$$

In dry acetone there is no possibility of the appearance of the proton coupled electron transfer pathway, labeled "H-atom" in Scheme II. However, in aqueous solution, where the Ru(II) reductant has a bound aqua ligand, the more facile H-atom pathway dominates and there is no sign of formation of the highly colored oxo-bridge dimer.

The energetic factors which make the outer-sphere pathway disadvantageous have already been discussed. However, an outer-sphere pathway does exist but it is not competitive with H-atom transfer. Furthermore, the H-atom transfer pathway is accessible only because of the special nature of the reactants—the $Ru^{IV}{=}O$ site is an electron–proton acceptor and the $Ru^{II}{-}OH_2$ site is an electron–proton donor. With less adequately constituted reactant partners or, for example, at a solid electrode, the outer-sphere pathway may be the *only accessible pathway* leading to relatively slow electron-transfer kinetics.

The mechanism for the H-atom pathway must involve initial preassociation of the reactants followed by the critical redox step.

Scheme III

$$b_2(py)Ru^{IV}{=}O^{2+} + b_2(py)Ru^{II}{-}OH_2^{2+} \underset{}{\overset{K_A}{\rightleftharpoons}} b_2(py)Ru^{IV}{=}O^{2+},H{-}O(H){-}Ru^{II}b_2(py)^{2+}$$

$$b_2(py)Ru^{IV}{=}O^{2+},H{-}O(H){-}Ru^{II}b_2(py)^{2+} \xrightarrow{k} b_2(py)Ru^{III}{-}OH^{2+},HO{-}Ru^{III}b_2(py)^{2+}$$

$$b_2(py)Ru^{III}{-}OH^{2+},HO{-}Ru^{III}b_2(py)^{2+} \xrightarrow{\text{rapid}} 2b_2(py)Ru^{III}{-}OH^{2+}$$

(b = 2,2′-bipyridine)

An estimate for the magnitude of the preassociation equilibrium constant, K_A, for two spherical reactants is available from the Eigen-Fuoss equation

$$K_A = \frac{4\pi N_0 d_3}{3000}\exp(-w_r/RT) \tag{18}$$

where d is the separation between reactants (Å), N_0 is Avagadro's number, and w_r is the electrostatic contribution to the free energy for bringing together the two reactants.[26] However, the rather severe structural constraints associated with the proton coupled electron transfer step must necessarily impose a considerable element of orientational demand as well which will appear in the experimentally observed rate constant and in the activation parameters for the reaction. On the basis of Scheme III, the experimentally observed rate constant is given by

$$k_f = k_{et}K_a' \tag{19}$$

where the statistical factor associated with the required relative orientation of the reactants for occurrence of the proton coupled electron transfer is included in K_a'.

There is another factor which may complicate the preassociation step. From the X-ray crystallographic work of Bino et al. on hydroxo/aqua complexes,[31] it appears that there is a special stability associated with H-bonding between coordinated hydroxo and aqua groups

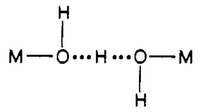

$$M{-}\overset{\overset{\displaystyle H}{|}}{O}\cdots H\cdots\underset{\underset{\displaystyle H}{|}}{O}{-}M$$

at least in the solid state. It is conceivable that a related interaction exists in solution between $Ru^{IV}{=}O^{2+}$ and $Ru^{II}{-}OH_2^{2+}$ as

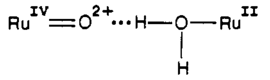

$$Ru^{IV}{=}O^{2+}\cdots H{-}\underset{\underset{\displaystyle H}{|}}{O}{-}Ru^{II}$$

prior to H-atom transfer. However, there is no evidence for protonation of the oxo complex even in strongly acidic media, and it is the electron transfer component of the "proton coupled electron transfer" act that *creates a proton affinity* at the Ru(IV) site.

The evidence suggesting that there is a concerted proton–electron transfer in the redox step has been presented above. For convenience this pathway is described here as H-atom transfer although it is important to note that in no sense of the phrase is there a literal transfer of an H-atom between the reactants. If a discrete H-atom were formed on a time scale long enough to reach thermal equilibrium with the surrounding medium

$$b_2(py)Ru^{IV}{=}O^{2+},H{-}O(H){-}Ru^{II}b_2(py)^{2+} \rightarrow b_2(py)Ru^{IV}{=}O^{2+},H,O(H){-}Ru^{III}b_2(py)^{2+} \tag{20a}$$

and then transferred

$$b_2(py)Ru^{IV}{=}O^{2+},H,O(H){-}Ru^{III}b_2(py)^{2+} \xrightarrow{\text{rapid}} b_2(py)Ru^{III}{-}OH^{2+},O(H){-}Ru^{III}b_2(py)^{2+} \tag{20b}$$

the net energy cost would be prohibitive. From redox potentials for the $[Ru^{III}(bpy)_2(py)(OH)]^{2+}/[Ru^{II}(bpy)_2(OH_2)]^{2+}$ and $H^+/H^\bullet$ couples,[32] the free energy for reaction 20a at pH 7 is $\Delta G° \simeq 64$ kcal mol^{-1}. Rather, the key redox step is a complex event at the molecular level involving significant electronic–vibrational coupling and only in the net sense are the elements of an H-atom transfer, one electron–one proton, transferred from one redox site to another.

There is sufficient information available to discuss the nature of the redox step in some detail. Electronically, the Ru(IV) acceptor site, $[Ru^{IV}(bpy)_2(py)(O)]^{2+}$, is a ground state magnetic singlet with a low-lying triplet.[33] In the triplet state there is single electron occupation of each of a degenerate or nearly degenerate pair of $d\pi$ levels, d_{xz} and d_{yz} in an axis system where the z-axis lies along the Ru═O bond. The $d\pi$ acceptor levels must be strongly mixed with filled p_x and p_y orbitals of the oxo ligand given the infrared evidence for multiple Ru-O bonding ($\nu_{Ru=O}$ = 792

---

[30] Baumann, J. A.; Meyer, T. J. *Inorg. Chem.* **1980**, *19*, 345.

[31] Bino, A. *Coord. Chem. Rev.*, in press.

[32] Latimer, W. M. *Oxidation Potentials*, 2nd ed.; Prentice-Hall: Englewood Cliffs, NJ, 1952; Chapter 3.

[33] Dobson, J. C.; Hatfield, W.; Meyer, T. J., work in progress.

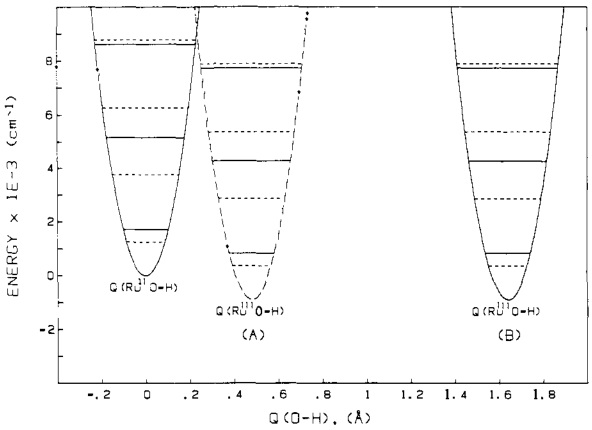

Figure 9. Harmonic oscillator description of the ν_{OH} modes for the reactants (Ru^{II}-OH) and products (Ru^{III}-OH) of the comproportionation reaction neglecting electronic coupling. The H-atom tunneling distance for H-bonded closest approach, case A, is $\Delta Q_{eq} \simeq 0.5$ Å, while reaction from van der Waals contact, case B, implies $\Delta Q_{eq} \simeq 1.6$ Å.

cm^{-1}).[1] Some of the most significant features of the redox step must be as follows: (1) There is no apparent basis for strong electronic coupling between the reactants in the association complex, $[Ru^{IV}{=}O,H{-}O(H){-}Ru^{II}]^{4+}$, or initial redox products, $[Ru^{III}{-}OH,O(H){-}Ru^{III}]^{4+}$, since there is no ligand sharing between redox sites. Interactions between redox sites are constrained to occur between the outer coordination spheres. The electron transfer component of the redox step involves the transfer of an electron from one of the filled $d\pi$ orbitals at the $(d\pi)^6$ Ru(II) site to d_{xz} or d_{yz} at Ru(IV). (2) There is no spin prohibition to the net reaction, whether it involves the magnetic singlet or triplet states of $Ru^{IV}{=}O^{2+}$. (3) Strong $\nu_{OH}(Ru^{II})$ vibrationally induced electronic coupling between the $d\pi$ Ru(II) and $d\pi$ Ru(IV) states must be an important feature of the redox step. Arguing as Endicott et al. have done for inner-sphere reactions,[34] a measure of the extent of electronic coupling is available from the energy difference between the intermediate state involving the appearance of a free H-atom, $[Ru^{IV}{=}O,H,HO{-}Ru^{III}]^{4+}$ ($\simeq$64 kcal mol^{-1} for reaction 20a), and the experimental activation energy ($E_a(H_2O) \simeq 3$ kcal mol^{-1}). The intermediate H-atom state is a useful reference state for the limit of no electronic coupling. The magnitude of the implied $\nu_{OH}(Ru^{II})$ vibrationally induced electronic coupling between d_{xz},d_{yz} (Ru^{IV}), 1s (H), and $d\pi$ (Ru^{II}) is impressive. (4) In contrast to electron transfer, the *simultaneous* transfer of both an electron and a proton involves *no net charge transfer component* and, therefore, no contribution to the activational requirements arising from the reorientation of solvent dipoles. (5) In the $Ru^{IV}{=}O$ oxidant *the electron and proton acceptor roles are at different sites* in the molecule with Ru(IV) being the electron acceptor and the oxo ligand the proton acceptor.

It is illustrative to consider the energetics of the redox step based on the normal coordinate–potential energy diagram in Figure 9. The most important vibrational contributions to the reaction must come from both ν_{Ru-O}, which decreases >400 cm^{-1} from $Ru^{IV}{=}O^{2+}$ to $Ru^{III}{-}OH^{2+}$,[1] and obviously ν_{OH} at Ru(II). The coordinate describing the H-atom transfer can be constructed from a linear combination of the $\nu_{OH}(Ru^{II})$ and $\nu_{OH}(Ru^{III})$ normal modes of the reactants and products. The potential energy curves in Figure 9 were constructed by using the harmonic oscillator approximation with force constants k(O–H) = 6.61 mdyn $Å^{-1}$ and a vibrational spacing of 3450 cm^{-1}.[23] For the deuterated case, shown as the dashed lines, the vibrational spacing is 2510 cm^{-1}, based on the greater reduced mass. The tunnelling distance for the H-atom transfer was calculated as the difference between the RuO—H bond length ($\simeq$0.96 Å) and the RuOH···O=Ru contact distance. Two limiting cases are shown in Figure 9 with case A representing the closest known (O···O) distance of $\simeq$2.4 Å in strongly hydrogen bonded systems,[35] [RuOH···O=Ru = 1.44 Å, ΔQ_{eq}(O—H) = 0.48 Å], while case B is for reaction from van der Waal's contact at a RuOH···O=Ru distance of $\simeq$2.6 Å,[35] [(O···O) = 3.6 Å, ΔQ_{eq}(O—H) = 1.64 Å]. The energy difference between the bottoms of the potential curves in Figure 9 was taken to be that for the overall reaction, $\Delta G° = -0.11$ V (-890 cm^{-1}).

The potential energy curves in Figure 9 illustrate the case of *no electronic coupling* between redox sites. Even at the closest possible approach between reactants, case A, there is a remarkable difference between the observed energy of activation ($E_a \simeq 1050$ cm^{-1}) and that predicted classically for the contribution to E_a from ν_{OH} at the intersection between the curves ($\simeq$7400 cm^{-1}). Clearly, vibrationally induced electronic coupling must play an important role in the reaction. A complete description of the ν_{OH} reaction coordinate must include the effects of nuclear motions on the extent of electronic coupling between the two redox sites and, hence, on the shape of the potential curves. In particular, the role of $\nu_{Ru=O}$ (792 cm^{-1}) induced electronic coupling requires consideration since the $v = 1$ vibrational level is thermally accessible.

The H/D kinetic isotope effect and its temperature dependence are also important characteristics of the reaction. The temperature dependences of isotope effects have been treated both in general and for simple outer-sphere reactions where electronic coupling is weak.[26,36] Quantum mechanically, electron transfer occurs as a non-radiative transition from the vibrational levels of the reactants to the vibrational levels of the products. The rate constant for electron transfer depends on the magnitude of the overlap between the vibrational wave functions for the reactants and products. For the same vibrational quantum number, vibrational overlaps for O–D vibrations lie lower in the potential energy curve than for O–H vibrations. The larger apparent E_a in D_2O compared with H_2O suggests that when the effects of electronic coupling are included there is an advantage in the deuterium case for thermal population of higher, electronically coupled levels where vibrational overlaps are larger. Because of the temperature dependence of k_{H_2O}/k_{D_2O}, the H/D kinetic isotope effect increases with decreasing temperature. Although not experimentally accessible, at very low temperatures where transitions occur only from $v = 0$ levels, the H/D kinetic isotope effect would be maximized and there would be no contribution to E_a from ν_{OH}. The low temperature isotope effects could be *considerably* greater than the value obtained here near room temperature. For example, in recent work a temperature independent isotope effect of $\simeq$50 was observed in the oxidation of benzyl alcohol by $[Ru^{IV}(bpy)_2(py)(O)]^{2+}$.[37]

The Cross Reaction. As for the comproportionation reaction, kinetic studies show that the cross reaction between $[Ru^{III}(trpy)(bpy)(OH)]^{2+}$ and $[Ru^{II}(bpy)_2(py)(OH_2)]^{2+}$ also occurs by two pathways which differ in their pH dependences. The first pathway, which is dominant for 3 < pH < 9, is pH independent and the reaction is

$$(trpy)(bpy)Ru^{III}{-}OH^{2+} + (bpy)_2(py)Ru^{II}{-}OH_2^{2+} \rightarrow (trpy)(bpy)Ru^{II}{-}OH_2^{2+} + (bpy)_2(py)Ru^{III}{-}OH^{2+} \quad (21)$$

$$(\Delta E°' = 0.056 \text{ V})$$

The pH dependence of the observed rate constant (Figure 6) is consistent with a second pathway involving $[Ru^{II}(bpy)_2(py)(OH)]^{+}$ as the reductant

$$(trpy)(bpy)Ru^{III}{-}OH^{2+} + (bpy)_2(py)Ru^{II}{-}OH^{+} \rightarrow (trpy)(bpy)Ru^{II}{-}OH^{+} + (bpy)_2(py)Ru^{III}{-}OH^{2+} \quad (22)$$

$$(\Delta E°' \simeq 0.134 \text{ V})$$

In contrast to the comproportionation reaction where $[k_{OH}/k_{H_2O}]^{25°C} = 0.114$, there is a *marked enhancement* of k_{OH} over k_{H_2O} for the cross reaction with $[k_{OH}/k_{H_2O}]^{25°C} = 110$. The rate enhancement dramatically illustrates the role of proton content

---

[34] Endicott, J. *Prog. Inorg. Chem.* **1983**, *30*, 141.

[35] (a) *The Hydrogen Bond Project*, HBS-100. 1975, Institute of Chemistry, University of Uppsala. Sweden. (b) Gordon, A. J.; Ford, R. A. *The Chemist's Companion*; Wiley-Interscience: New York, 1972; pp 107–115.

[36] Buhks, E.; Bixon, M.; Jortner, J. *J. Phys. Chem.* **1981**, *85*, 3763.

[37] Roecker, L.; Meyer, T. J. *J. Am. Chem. Soc.* **1987**, *109*, 746.

in determining both the observed rate and the mechanism. When there is no change in proton content between reactants and products as in reaction 22, a "normal" outer-sphere pathway exists without the intervention of any high-energy intermediates, and the observed rate constant approaches that expected from related studies on self-exchange reactions of polypyridyl complexes of ruthenium.

For pH <1, where $[\mathrm{Ru^{III}(trpy)(bpy)(OH_2)}]^{3+}$ ($\mathrm{p}K_{a1} \simeq 1.7$) and $[\mathrm{Ru^{III}(bpy)_2(py)(OH_2)}]^{3+}$ ($\mathrm{p}K_{a1} = 0.85$) become the dominant forms of Ru(III), a similar outer-sphere pathway would be expected to exist between the aqua ions of the two complexes

$$\mathrm{(trpy)(bpy)Ru^{III}{-}OH_2^{3+} + (bpy)_2(py)Ru^{II}{-}OH_2^{2+} \rightarrow (trpy)(bpy)Ru^{II}{-}OH_2^{2+} + (bpy)_2(py)Ru^{III}{-}OH_2^{3+}} \quad (23)$$

Presumably, if kinetic studies had been feasible at the higher ionic strengths required to reach this pH domain then an additional, relatively rapid pathway (eq 23) would also have appeared.

Although not well defined, due to limited experimental data, the H/D kinetic isotope effect (k_{OH}/k_{OD}) $\simeq$ 1.5 (25 °C, $I = 0.005$ M) for the k_{OH} pathway of the cross reaction is quite small, consistent with an outer-sphere mechanism.[23,36] Although less dramatic than for the comproportionation reaction, the H/D kinetic isotope effect for the k_{H_2O} pathway (k_{H_2O}/k_{D_2O}) = 5.8 (25 °C, $I = 0.005$ M) is still significant. As shown by the data in Figure 7, the dependence of k_{H_2O} on mole fraction of deuterium is also linear, within experimental error, suggesting the participation of a single proton site in the redox step. As for the comproportionation reaction, a mechanism involving initial outer-sphere electron transfer

$$\mathrm{(trpy)(bpy)Ru^{III}{-}OH^{2+} + (bpy)_2(py)Ru^{II}{-}OH_2^{2+} \rightarrow (trpy)(bpy)Ru^{II}{-}OH^{+} + (bpy)_2(py)Ru^{III}{-}OH_2^{3+}} \quad (24a)$$

followed by rapid H^+ transfer steps

$$\mathrm{(trpy)(bpy)Ru^{II}{-}OH^{+} + H^{+} \rightarrow (trpy)(bpy)Ru^{II}{-}OH_2^{2+}} \quad (24b)$$

$$\mathrm{(bpy)_2(py)Ru^{III}{-}OH_2^{3+} \rightarrow (bpy)_2(py)Ru^{III}{-}OH^{2+} + H^{+}} \quad (24c)$$

can apparently be ruled out on energetic grounds. By analogy with eq 15a,b, ΔG for the initial outer-sphere electron transfer step can be calculated from the expression

$$\Delta G^{\circ\prime}_{os} = -RT \log_e \left\{ \frac{K_{a1}(\mathrm{II})}{K_{a1}'(\mathrm{III})} \right\} + \Delta G^{\circ\prime}_{rxn} \quad (25)$$

From $\Delta G^{\circ\prime}_{rxn} = -1.3$ kcal mol^{-1} and the K_{a1} values for the aqua ions, $[\mathrm{Ru^{II}(trpy)(bpy)(OH_2)}]^{2+}$ ($\mathrm{p}K_{a1} = 9.7$)[2a] and $[\mathrm{Ru^{III}(bpy)_2(py)(OH_2)}]^{3+}$ ($\mathrm{p}K_{a1}' = 0.85$),[1] $\Delta G^{\circ\prime}_{os} \simeq +11$ kcal mol^{-1}, giving the *maximum* rate constant $k \simeq 7.5 \times 10^4$ M^{-1} s^{-1}, which is significantly less than the experimentally observed value of $k_{H_2O} = 4.0 \times 10^5$ M^{-1} s^{-1}. In D_2O solution, where the value of $k_{D_2O} = 7.06 \times 10^4$ M^{-1} s^{-1}, it is possible that the outer-sphere pathway may contribute to the observed rate, producing the lower value of the kinetic isotope effect than found for the comproportionation reaction.

However, in H_2O it appears that the cross reaction must occur by a "proton assisted electron transfer" or H-atom transfer mechanism, Scheme IV, in order to avoid the proton composition dilemma imposed by simple outer-sphere electron transfer.

Scheme IV

$$\mathrm{(trpy)(bpy)Ru^{III}(OH)^{2+} + (bpy)_2(py)Ru^{II}(OH_2)^{2+} \overset{K_A'}{\rightleftharpoons} (trpy)(bpy)Ru^{III}{-}(H)O^{2+},H{-}O(H){-}Ru^{II}(bpy)_2(py)^{2+}}$$

$$\mathrm{(trpy)(bpy)Ru^{III}{-}(H)O^{2+},H{-}O(H){-}Ru^{II}(bpy)_2(py)^{2+} \xrightarrow{k} (trpy)(bpy)Ru^{II}{-}(H)O{-}H^{2+},O(H){-}Ru^{III}(bpy)_2(py)^{2+}}$$

$$\mathrm{(trpy)(bpy)Ru^{II}{-}(H)O{-}H^{2+},O(H){-}Ru^{III}(bpy)_2(py)^{2+} \xrightarrow{rapid} (trpy)(bpy)Ru^{II}(OH_2)^{2+} + (bpy)_2(py)Ru^{III}(OH)^{2+}}$$

Scheme V

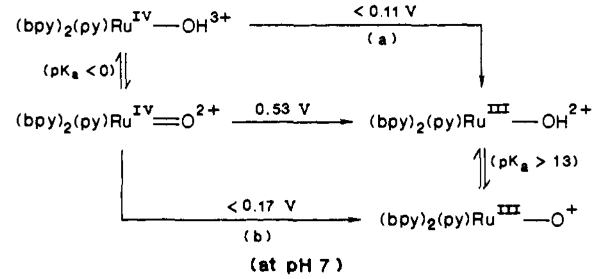

In comparing the apparently analogous pathways for comproportionation and the cross reaction, there are some clear similarities and some notable differences: (1) Although there is no basis for strong electronic coupling between the reactants or initial products, because of the absence of ligand sharing between coordination spheres, strong ν_{OH} induced electronic coupling must play an important role in the reaction. In this case the possibility exists for a significant H-bonding interaction via

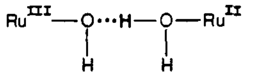

$$\mathrm{Ru^{III}{-}O(H)\cdots H{-}O(H){-}Ru^{II}}$$

precursor complexes.[31] In principle, a mixed-valence structure of this type could exist in a "delocalized" state

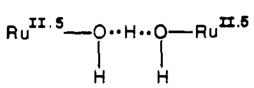

$$\mathrm{Ru^{II.5}{-}O(H)\cdots H\cdots O(H){-}Ru^{II.5}}$$

In the more usual ligand-bridged mixed-valence dimers the extent of electronic coupling plays a critical role in determining the extent of delocalization. However, in the outer-sphere, H-bonded case, the key is the influence of the O···H—O bond distance change on the electronic coupling between sites. (2) While variations in solvent or ionic strength may influence the equilibrium preassociation between the reactants, they are not expected to influence the rate of the redox step in any significant way due to the H^+/e^- coupled nature of the redox process. (3) Although the origin of the H/D isotope effect lies in $\Delta H^{\ddagger}$ (E_a) for both the comproportionation and cross reactions, the actual pattern of activation parameters is quite different. For the cross reaction both $\Delta H^{\ddagger}$ (E_a) and $\Delta S^{\ddagger}$ (A) are considerably larger. A detailed interpretation of the origin of these variations is beyond our capabilities at present, but it may be a reflection of better electronic-vibrational wave function overlap in levels above $v = 0$, giving the reactions more of an appearance of classical activated complex behavior.

Implications for Electron Transfer in Related Systems. The issues raised here concerning the role of protons in the electron transfer reactions of aqua ions are of general applicability and must unavoidably dictate their redox characteristics. A particular example is the common observation that for outer-sphere reactions such as the oxidation of $[\mathrm{Ru(NH_3)_6}]^{2+}$ by $[\mathrm{Fe^{III}(H_2O)_6}]^{3+}$ and its conjugate base $[\mathrm{Fe^{III}(H_2O)_5(OH)}]^{2+}$ in acidic solution the rate is diminished for the conjugate base compared with $[\mathrm{Fe(H_2O)_6}]^{3+}$.[38] The explanation lies in the relative thermodynamic disadvantage of forming in the initial outer-sphere electron transfer step the conjugate base of the lower oxidation state, e.g., $[\mathrm{Fe^{II}(H_2O)_5(OH)}]^{+}$. For an outer-sphere pathway, if there is a change in proton content between the different oxidation states of a couple such a rate inhibition *will always exist*. This necessarily includes many electrochemical reactions at metal electrodes involving aqua ions and helps to explain why the heterogeneous charge transfer kinetics for such couples can be slow. The point is illustrated in Scheme V with use of the $[\mathrm{Ru^{IV}(bpy)_2(py)(O)}]^{2+}/[\mathrm{Ru^{III}(bpy)_2(py)(OH)}]^{2+}$ couple at pH 7 as the example. If reduction of Ru(IV) to Ru(III) occurs either by outer-sphere electron transfer followed by proton gain (path b in Scheme V) or initial proton gain followed by electron transfer (path a in Scheme 5), high-energy intermediates with regard to proton content are necessarily

J. Am. Chem. Soc. **1987**, *109*, 3297-3301

involved. In path b the potential of the Ru(IV)/(III) couple is reduced because Ru(III) is formed in a non-equilibrium proton composition. In path a the potential is reduced because of the low equilibrium concentration of the protonated oxo complex. The problem is less severe for the Ru(III)/(II) couple where the relevant pK_a values are ~1 for $[Ru^{III}(bpy)_2(py)(OH_2)]^{3+}$ and ~11 for $[Ru^{II}(bpy)_2(py)(OH_2)]^{2+}$.

The "proton assisted electron transfer" or H-atom transfer pathway discussed here represents at least a partial solution to the dilemma posed by changes in proton content accompanying electron transfer. However, it is mechanistically more complex than outer-sphere electron transfer and as shown, for example, by reactions between $[Ru^{IV}(bpy)_2(py)(O)]^{2+}$ and $[Ru^{II}(bpy)_2(py)(OH_2)]^{2+}$ (eq 12) compared with $[Ru^{IV}(bpy)_2(py)(O)]^{2+}$ and $[Ru^{II}(bpy)_2(py)(OH)]^{+}$ (eq 13) or between $[Ru^{III}(trpy)(bpy)(OH)]^{2+}$ and $[Ru^{II}(bpy)_2(py)(OH_2)]^{2+}$ (eq 21) compared with $[Ru^{III}(trpy)(bpy)(OH)]^{2+}$ and $[Ru^{II}(bpy)_2(py)(OH)]^{+}$ (eq 22), will probably only play an important role for those cases where the difference between reactants is one proton and one electron, i.e., an H-atom. Where such pathways appear, as indicated by appreciable H/D kinetic isotope effects, the term "H-atom transfer" refers to what is *transferred* between reactants in the net sense and *not to the mechanism* of the event. The details of the mechanisms involved are necessarily complex, involving time dependent electronic–vibrational coupling events which demand a quantum mechanical description in the limit where the Born–Oppenheimer approximation is no longer valid.

In some cases H-atom transfer may not be competitive with an initial outer-sphere electron transfer step followed by proton transfer. H-atom transfer pathways have been invoked previously, most notably for the $[Fe(H_2O)_6]^{3+/2+}$ self-exchange reaction which displays a relatively small H/D kinetic isotope effect.[39] Although the small isotope effect can be explained as a secondary effect on an outer-sphere mechanism,[29a] there is other experimental evidence for the existence of H-atom transfer pathways. For example, although outer-sphere oxidation of $[Ru(NH_3)_6]^{2+}$ by $[Fe^{III}(H_2O)_5(OH)]^{2+}$ is decreased by ≃6 compared with $[Fe^{III}(H_2O)_6]^{3+}$, the oxidation of $[Ru(NH_3)_5(OH_2)]^{2+}$ by $[Fe(H_2O)_5(OH)]^{2+}$ is *increased* by a factor of ≃6 compared with that of $[Fe(H_2O)_6]^{3+}$.[38] While the conventional interpretation of the origin of inverse acid terms in self-exchange reactions like $[Fe(H_2O)_6]^{3+/2+}$ is attributed to an inner-sphere pathway involving the redox partners $[Fe^{III}(H_2O)_5(OH)]^{2+}$ and $[Fe^{II}(H_2O)_6]^{2+}$, there is a clear possibility that such effects could have their origin in the H-atom transfer pathway, an issue that could be resolved by further studies in D_2O.

Acknowledgment is made to the National Science Foundation for support of this research (Grant CHE-8304230) and to Prof. J. K. Beattie of the University of Sydney for helpful discussions on the kinetics analysis.

Registry No. $Ru^{IV}(bpy)_2(py)(O)^{2+}$, 67202-43-1; $Ru^{II}(bpy)_2(py)(OH_2)^{2+}$, 70702-30-6; $Ru^{III}(trpy)(bpy)(OH)^{2+}$, 81971-63-3; D_2, 7782-39-0.

---

[38] Meyer, T. J.; Taube, H. *Inorg. Chem.* **1968**, *7*, 2369.

[39] (a) Horne, R. A. *J. Phys. Chem.* **1960**, *64*, 1512. (b) Hudis, J.; Dodson, R. W. *J. Am. Chem. Soc.* **1956**, *78*, 911. (c) Sutin, N.; Rowley, J. K.; Dodson, R. W. *J. Phys. Chem.* **1961**, *65*, 1248. (d) Fukushima, S.; Reynolds, W. L. *Talenta* **1964**, *11*, 283.

Electron and Energy Shuttling between Redox Sites on Soluble Polymers

John Olmsted III,*† Steven F. McClanahan,‡ Earl Danielson,‡ Janet N. Younathan,‡ and Thomas J. Meyer*‡

Contribution from the Department of Chemistry and Biochemistry, California State University, Fullerton, California 92634, and the Department of Chemistry, The University of North Carolina, Chapel Hill, North Carolina 27514.
Received November 7, 1986

Abstract: 9-Methylanthracene (9-MeAn) is found to function as an efficient, sequential energy and electron transfer shuttle between chromophore and redox sites bound to separate strands of chemically modified polystyrene. Sensitized formation of the triplet excited state, ^{3}(9-MeAn)*, occurs by energy transfer following visible irradiation of a polymer-bound polypyridyl complex of Ru(II), PS-(Ru^{II}). In the presence of separate polymers containing reductive (phenothiazene, PS-PTZ) or oxidative sites (paraquat, PS-PQ^{2+}), a series of subsequent electron transfer steps results in the transient generation of PS-$PTZ^{\cdot+}$ and PS-$PQ^{\cdot+}$ and the net photoinduced production and separation of oxidative and reductive equivalents on separated polymers. The rate of recombination between PS-$PQ^{\cdot+}$ and PS-$PTZ^{\cdot+}$ by back electron transfer is reduced by a factor of 27 relative to an analogous system based on PTZ and PQ^{2+} monomers.

Rapid "charge recombination" by back electron transfer imposes rather severe restrictions on any energy storage scheme based on electron transfer quenching of molecular excited states in solution, e.g., eq 2 followed by 3.[1] The recombination or back electron transfer step is a bimolecular process, and it is possible to reduce its rate by modifying the microenvironment of the system such that diffusion is hindered. Several approaches for making such modifications have been explored, and the results are summarized in a recent review.[2] One strategy has been to anchor the donor and acceptor sites on separate polymeric strands, thereby reducing their mobility and decreasing the rate of recombination.[2-4] However, if polymeric attachment reduces the rate of recombination, it must also slow the second-order processes by which the

$$Ru(bpy)_3^{2+} \xrightarrow{h\nu} Ru(bpy)_3^{2+*} \qquad (1)$$

$$Ru(bpy)_3^{2+*} + PQ^{2+} \longrightarrow Ru(bpy)_3^{3+} + PQ^{\cdot+} \qquad (2)$$

$$Ru(bpy)_3^{3+} + PQ^{\cdot+} \longrightarrow Ru(bpy)_3^{2+} + PQ^{2+} \qquad (3)$$

(where bpy is 2,2′-bipyridine; PQ^{2+} is paraquat,

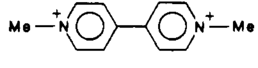

[†] California State University.

[‡] University of North Carolina.

[1] Bock, C. R.; Meyer, T. J.; Whitten, D. G. *J. Am. Chem. Soc.* **1974**, *96*, 4710.

[2] Rabani, J.; Sasson, R. E. *J. Photochem.* **1985**, *29*, 7.

[3] Sassoon, R. E.; Rabani, J. *J. Phys. Chem.* **1985**, *89*, 5500.

[4] Margerum, L. D.; Murray, R. W.; Meyer, T. J. *J. Phys. Chem.* **1986**, *90*, 7289

0002-7863/87/1509-3297$01.50/0 © 1987 American Chemical Society